PARAMETERIZATION AND STATISTICAL ANALYSIS OF HURRICANE WAVES

A Thesis

by

PATRICK WILLIAM MCLAUGHLIN

Submitted to the Office of Graduate and Professional Studies of
Texas A&M University
in partial fulfillment of the requirements for the degree of

MASTER OF SCIENCE

Chair of Committee,	James M. Kaihatu
Committee Members,	Steven F. DiMarco
	Francisco Olivera
Head of Department,	Robin L. Autenreith

May 2014

Major Subject: Ocean Engineering

ABSTRACT

Recently, Gulf coast communities have experienced significant damage from landfalling hurricanes. While the effects of hurricane surge on coastal communities have been examined and better defined, risk of damage due to hurricane waves is less quantified. This thesis presents the Wave Response Function (WRF) methodology. Hurricanes are parameterized in the form of non-dimensional equations incorporating key physical hurricane parameters. The non-dimensional equations are then combined with a fully developed sea state cap (Young and Verhagan 1996) to form the open coast and bay methodologies. This approach yields root mean square errors (RMSE) ranging from 0.01-0.46 m, with the majority of points below 0.3 m. This approach yields small bias values. The WRF method was compared to Hurricane Ike data (Kennedy et al. 2011) and yielded RMSE of 0.67 meters despite the higher depths of the recording stations. The WRF method was also compared to Taylor's (2012) parameterized wave equations, with mean RMSE improvements ranging from 0.13-0.32 m.

Once WRF coefficients are adjust to minimize RMSE at each station under consideration, extreme value analysis via the Joint Probability Method with Optimal Sampling (JPM-OS) was conducted. When applied to Panama City, FL the JPM-OS methodology yielded extreme value statistics for 179 stations of interest. Maps detailing the spatial extents of the 100 and 1000 year maximum wave event were created using ArcGIS.

DEDICATION

I would like to dedicate this thesis to my parents William and Susan McLaughlin. Your support and love throughout my life has been never ending. Thank you for everything that you've given me.

ACKNOWLEDGEMENTS

I would like to thank my committee chair, Dr. James Kaihatu, for his continual guidance throughout my time here at Texas A&M. I would also like to thank Dr. Francisco Olivera, and Dr. Steven DiMarco for their contributions reviewing this thesis. I am very grateful to Dr. Jennifer Irish and Nick Taylor for their weekly brainstorming ideas that helped shape the work in this thesis. In addition, I would like to extend a special thanks to Dr. Ikpoto Udoh and Antonne Taylor, for answering my ADCIRC-SWAN questions and helping me get around computing roadblocks during my early time here at Texas A&M. I would like to thank my parents, Bill and Susan, and my sister Megan, for their undying support during my time in Texas. Their encouragement and love has made moving halfway across the country infinitely easier. Finally I would like to thank my friends, both here at A&M, from Villanova University, and back home from my early years at Coxsackie-Athens High school. No man is a failure who has friends.

TABLE OF CONTENTS

Page

ABSTRACT ii

DEDICATION iii

ACKNOWLEDGEMENTS iv

TABLE OF CONTENTS v

LIST OF FIGURES vii

LIST OF TABLES x

1. INTRODUCTION 1

    1.1 Hurricane Hazards and Historical Examples 1
    1.2 Motivation 2
    1.3 Research Objectives 4

2. LITERATURE REVIEW 6

    2.1 Hurricane Wave Generation and Overview 6
        2.1.1 Surge Generation 6
        2.1.2 Hurricane Wave Fields 7
        2.1.3 Fully Developed Sea States 9
    2.2 Applications of Hurricane Wave Modeling 11
    2.3 Extreme Value Statistics of Hurricanes 12
    2.4 Parameterized Wave Models 13

3. NUMERICAL MODELS AND SITE OVERVIEW 17

    3.1 Model Details 17
        3.1.1 Advanced Circulation Model (ADCIRC) 17
        3.1.2 Simulating Waves Near shore (SWAN) 20
        3.1.3 Steady-State Spectral Wave Model (STWAVE) 21
        3.1.4 Planetary Boundary Layer (PBL) Model 22
        3.1.5 Coupling of ADCIRC-SWAN and ADCIRC-STWAVE 23
    3.2 Simulation Area 25

4. WAVE RESPONSE FUNCTION DEVELOPMENT AND ANALYSIS 33

4.1 Introduction to Development 33
4.1.1 Parameter Selection 33
4.1.2 Application of the Non-dimensional Formulation 43
4.1.3 Addition of a Fully-Developed Sea State Cap to Methodology 46
4.1.4 Bay Station WRF Methodology and Application 49
4.1.5 Open Coast WRF Methodology and Application 58
4.2 Taylor (2012) Comparison and Hurricane Ike Data Validation 64
4.3 Conclusions of WRF Parameterization Study 68

5. WRF APPLICATION TO EXTREME VALUE STATISTICS 70

5.1 JPM-OS: Methodology and Surge Application 70
5.2 JPM-OS Application to Panama City, FL Waves 76
5.3 Projecting Wave Heights onto Land for ArcGIS Analysis 82

6. SUMMARY AND CONCLUSIONS 92

REFERENCES 94

LIST OF FIGURES

		Page
Figure 2.1	Schematic of wave generation within a moving hurricane. …….	8
Figure 3.1	Location of the three study sites along the Gulf Coast as well as enlarged satellite photos of each site. Site name counter-clockwise from upper left : Corpus Christi, TX, Gulfport, MS, Panama City, FL.	26
Figure 3.2	WRF Station locations for Corpus Christi, TX. All 159 stations shown, with 30 bay stations and 129 bay stations delineated by color.	28
Figure 3.3	WRF Station location and map of surrounding area for Gulfport, MS. 70 O.C. stations shown in red and 95 Bay stations shown in green. Note: Bay of St. Louis located on Western side of map, while Biloxi Bay is to the East.	30
Figure 3.4.	All 346 WRF stations shown for Panama City, FL. 74 Open Coast stations shown in red and 272 bay stations shown in green.	31
Figure 4.1	Time series for Open Coast station #47. Note that maximum wave event (vertical red line) occurs 1 hour after maximum surge event (vertical blue line).	37
Figure 4.2	Time series for: Top- Bay station #25 (Bay of St. Louis), and Bottom- Bay station #125 (Biloxi Bay). Maximum wave events (vertical red line) occur after maximum surge events (vertical blue line) for both stations.	38
Figure 4.3	Example of different categories of storms for each type of fitting. Left, Middle, and Right storms grouped together. Example storm tracks shown for each category of storm.	41
Figure 4.4	Fitting examples for all three test sites. Site Names from top to bottom: Gulfport, MS, Panama City, FL, Corpus Christi, TX. Red lines represent storms making landfall to the right, green to the left, and blue in the middle of the suit of WRF points. For reference, fitting colors correspond to example storms in Fig. 4.1.	42

Figure 4.5 Back Prediction at open coast station # 47 (Top) and bay station #25 (bottom). Color coding as follows: Green- storms that make landfall to the left (West) of the WRF points; Blue- storms that make landfall in the middle of the WRF points; Red- storms that make landfall to the right (East) of the WRF points. 45

Figure 4.6 Comparison of wave heights predicted by: Model (blue), fully developed equations (red), and non-dimensional equations green. 52

Figure 4.7 Clockwise from upper left: Bay of St. Louis RMSE (m), Biloxi Bay RMSE (m), Biloxi Bay Percent error, Bay of St. Louis Percent error. 55

Figure 4.8 Left to right: Percent error at Corpus Christi, TX bay stations, RMSE error at bay stations 56

Figure 4.9 Left to right: Percent error at Panama City, FL bay locations, RMSE (m) at bay locations. 57

Figure 4.10 Spatial distribution of percent error (left) and RMSE in meters (right) at Panama City, FL open coast stations. 61

Figure 4.11 Spatial distribution of percent error (left) and RMSE in meters (right) at Panama City, FL open coast stations. 62

Figure 4.12 Spatial distribution of percent error (left) and RMSE in meters (right) at Panama City, FL open coast stations. …….. 63

Figure 4.13 Back prediction results from the WRF method (Y-axis) vs recorded Kennedy et al. (2011) maximum significant wave heights (m). RMSE =0.67 (m). 67

Figure 5.1 Surge return period curves for bay and open coast stations. Top row shows open coast stations 1 and 15, while bottom row shows bay stations 26 and 165. 75

Figure 5.2 Wave return period curves for bay and open coast stations. Top row shows open coast stations 1 and 15, while bottom row shows bay stations 26 and 165. Note the significantly lower bay wave heights when compared to the surge curves seen in Fig. 5.1. 78

Figure 5.3 100 year maximum significant wave height for all Panama City, FL stations. ……..... 81

Figure 5.4 Thiessen polygons for shoreline watershed delineation. Application to Corpus Christi, TX. Figure and method by PhD student Chih-Hung Hsu (AaronHsu@tamu.edu). ..…..… 83

Figure 5.5 SRF zones for Panama City, FL. Each zone has a corresponding station where surge data is calculated and distributed through the zone using the Hsu methodology. 84

Figure 5.6 Percentage of overlapping storm events between 100 year surge and wave events, determined by analyzing JPM storm inputs. Analyzed for all storms within 10 % (left) and 20 % (right) of the 100 year level. Shown for all storm parameters (black) and excluding x_o parameter. 87

Figure 5.7 Spatial map of 100 year maximum significant wave height over land areas for Panama City, FL. 90

Figure 5.8 Spatial map of 1000 year maximum significant wave height over land areas for Panama City, FL. 91

LIST OF TABLES

Page

Table 4.1 RMSE's at all bay stations. 44

Table 4.2 RMSE's at all open coast stations 44

Table 4.3 RMSE's averaged across all bay stations for Non-dimensional and Combined methods described above. 51

Table 4.4 Basic statistics for all sites, averaged across all bay stations. 53

Table 4.5 RMSE (m) for methods (1-3) described above, averaged over all open coast stations at each location. 59

Table 4.6 Basic stats for all sites, averaged across all open coast stations. 60

Table 4.7 Summary of RMSE m averaged over all stations from the Taylor (2012) method and the WRF method discussed in this study. Improvement (m) from Taylor (2012) shown in last column 64

Table 5.1 Resolution chosen for each parameter used in JPM-OS calculations. Format is as follows: (minimum value:step:maximum value) 73

Table 5.2 Maximum surge and wave levels seen for 50, 100, and 500 year return periods, split by bay (top) and open coast (bottom) locations. 79

Table 5.3 Return period equivalent for +/- 10% of 100 year surge level. 88

Table 5.4. Return period equivalent for +/- 10% of 100 year wave level. 88

1. INTRODUCTION

1.1 Hurricane Hazards and Historical Examples

Hurricanes are one of the most destructive, pertinent natural disasters affecting coastal communities along the United States shoreline. Hurricanes are tropical cyclones with maximum sustained surface winds of 74 mph (Taylor and Hebert 1978). These storms have the potential to cause catastrophic damage to coastal communities and industries. The 1900 Galveston Hurricane still remains the most deadly natural disaster in United States history (NOAA 2012). Although coastal engineering structures and practices, along with public knowledge and preparation, have increased greatly since the deadly storm of 1900 made landfall, hurricanes are still a costly, destructive natural disaster whose damage has yet to be fully quantified. Recent hurricane events such as the 2004 and 2005 hurricane seasons saw seven of the ten costliest tropical cyclones in U.S. history, totaling 192 billion dollars in damage (Blake et al. 2011). Along the U.S. Gulf Coast, Hurricane Katrina caused 1,833 deaths, making it the most deadly storm event since the 1928 Okeechobee hurricane (Knabb et al. 2005). In addition to the extensive loss of life and property damage caused by Hurricane Katrina, it is estimated that Katrina may have caused upwards of $150 billion dollars total damage when economic impacts are considered. Katrina had a significant impact on the energy industry, with 30 oil platforms being damaged and forcing nine oil refineries to close (U.S. Department of Commerce 2006). One of the major reasons for the extensive

damage during hurricane Katrina was the high surge levels seen in low lying cities such as New Orleans, many areas of which are below sea level. The highest surge recorded during the storm was 8.47 m at Pass Christian, MS (Knabb et al. 2005). Other recent events such as Hurricanes Ike and Gustav (2008) caused widespread damage to the Gulf Coast, causing extensive damage to the economy and civilian properties.

1.2 Motivation

Typically, hurricane winds and the accompanying inundation due to elevated surge levels are regarded as the most damaging characteristics of landfalling hurricanes (Taylor and Hebert 1978). Numerous studies including Toro et al. (2010) and Niedoroda et al. (2010) have examined the damage caused by of storm surge inundation. Previous work including Irish et al. 2009, Irish and Resio (2010) , Song et al. (2012), and Udoh (2013) has examined the application of parameterized surge response functions, or SRF's, to hurricane surge prediction. Further application of the SRFs to probabilistic extreme value analysis was conducted in Resio et al. (2009) and Irish et al. (2011) have used the formulation of SRFs along with the Joint Probability Method with Optimum Sampling (JPM-OS), which will be examined in further detail in Section 5. The extreme value surge statistics generated by the JPM-OS method can be used as an essential component of coastal community planning and civil defense strategy development.

To date, there has been little quantification of near shore wave height extreme value statistics or consequent damage, particularly as linked to statistics of extreme weather. Recent work by Kennedy et al. (2011) and Tomzik et al. (2014) have attempted to assess and quantify hurricane induced wave damage. With these recent developments, it is possible to forecast damage scenarios given statistics on near shore surge levels and wave heights. Skillful predictions of hurricane forced near shore maximum wave heights, or $H_{s\,max}$, are therefore necessary for extreme value statistics and subsequent damage vulnerability assessments.

Current methods for predicting $H_{s\,max}$ involve high resolution numerical surge and wave models, such as the coupled ADCIRC-STWAVE or ADCIRC-SWAN models. These modeling systems require large computational times, limiting their usefulness when applied to the simulation of the thousands of storms necessary to analyze extreme value statistics using the JPM-OS methodology. Therefore, the translation of hurricane parameters to computationally efficient predictions of near shore $H_{s\,max}$ is essential to better quantify extreme value statistics for hurricane waves.

The parameterization of near shore H_s^{max} is part of a larger NOAA and Sea Grant funded study (Grant No. NA10OAR4170099) investigating the social and economic vulnerability of various coastal communities to hurricane forced surge and wave events. A similar surge parameterization and extreme value analysis following the methods of Resio et al. (2009), Song et al. (2012), and Irish et al. (2013) is currently being conducted by Dr. Jennifer Irish and Nicholas Taylor. Their surge results, combined with

the wave results presented in this thesis will be the basis for social and economic vulnerability analysis of Corpus Christi, TX, Gulfport, MS, and Panama City, FL.

1.3 Research Objectives

The ultimate goal of this work is to develop parameterized equations that accurately and efficiently predict maximum hurricane wave height in the near shore for a given set of hurricane parameters. This will be done using the Wave Response Function, or WRF, methodology developed in this study. A subsequent goal is to validate the WRF method for selected sites along the U.S. Gulf Coast to examine and help mitigate the error introduced. Typical Simulating Waves Nearshore (SWAN) model Root Mean Square Errors (RMSE) are around 0.30 m (Ris et al. 1999). This study aims to keep errors of the WRF method below 0.30 m, (the project RMSE) in order to avoid introducing any additional error into wave prediction. Finally, this work aims to apply the JPM-OS using the newly developed wave response functions, and extreme value wave statistics along the Gulf Coast. Once extreme value statistics are analyzed, this research aims to generate high resolution wave height maps for selected return period storms. Based on wave theory and hurricane wave height sensitivity testing conducted previously by Taylor (2012), we hypothesize that the effects of hurricane distance to landfall central pressure, total depth, and storm radius on wave height are significant. Consequently their inclusion in the WRFs developed during this work is paramount.

This thesis will show the development of the WRF methodology as well as results of extreme value analysis at selected bay and open coast locations.

The remainder of this thesis is organized as follows: discussion on related literature is presented in Section 2. Numerical model overview, extreme value analysis, study areas, are presented in Section 3. Section 4 discusses development of the wave response functions and application to the study areas outlined in Section 3. Section 5 includes the application of the WRF's to JPM-OS methodology, generation of extreme value statistics for selected stations, and high resolution maps of significant wave heights generated by selected return period storms. Finally, Section 6 discusses the major findings of this work, conclusions, and any related future research.

2. LITERATURE REVIEW

2.1 Hurricane Wave Generation and Overview

Aside from the effect of wind, dominant processes that affect wave heights in the near shore environment are shoaling, refraction, and depth induced breaking (Holthuijsen 2007). Rapidly turning hurricane wind fields contribute to the complex wave fields seen within and near a translating hurricane (Wright et al. 2001). The anticyclonic nature of hurricane winds create stresses on the water surface that have a significant effects on both wave and surge generation. Since methods in this study will examine waves in near shore environments, it is important to also understand surge generation, as near shore wave growth is an extremely depth dependent process.

2.1.1 Surge Generation

Storm surge is often treated as a long wave where the change in water level is caused by the hurricane winds blowing over long distances (Freeman et al. 1957). Frictional drag from hurricane winds causes wind shear stresses, τ_w, that act on the water surface, which is determined from

$$\tau_w = \rho k W |W| \tag{2.1}$$

where ρ is the density of water, k, is a dimensionless friction factor, W is the 10 m wind speed vector, and $|W|$ is the absolute value of the wind speed vector (Van Dorn 1953).

These wind shear stresses acting on the water surface cause a redistribution of water, pushing a previously offshore water mass towards the coast. When this redistributed water mass reaches the coast, a piling up of water occurs due to the presence of the coastline. The increased near shore water slope is explained by the equation

$$\frac{\partial \eta}{\partial x} = \frac{n\tau_{zx}(\eta)}{\rho g(h+\eta)} \tag{2.2}$$

Here n is a friction factor which includes bottom friction and wind shear stress, τ_{zx} is the wind stress at the water surface, h is the local water depth, and η is the change in water depth (Dean and Dalrymple 1991). It is apparent that as local water depth decreases, the slope of the incoming surge increases. As the displaced water reaches the near shore environment, the slope of the sea surface increases in accordance with Equation. (2.2) and the surge depth increases. This increased depth inundates previously dry areas in addition to allowing larger waves to propagate farther inland than under non-storm conditions.

2.1.2 Hurricane Wave fields

Quantification of the complex hurricane wave fields has been conducted through various methods including wave reports from ships (Arakawa and Suda 1953), in-situ buoy measurements during hurricane conditions (Panchang and Li 2006, Young 1998), and remote sensing data using synthetic aperture radar (SAR) (King and Shemdin 1978). These data observations are used to develop a conceptual model of the hurricane wave

field. Waves generated to the right of the storm center (northern hemisphere) approximately align with the wind vector in this region, are under the most intense winds for a longer duration, and are thus likely to be the most energetic waves generated. Conversely, waves generated to the left side of the storm (northern hemisphere) propagate against the direction of forward movement and spend less time in the area of intense winds (Young 2003). This causes an uneven spatial distribution of the wave field, which due to the constantly turning anticyclonic winds does not exactly mirror the wind field. Figure 2.1, from Young (2003) provides a visualization of the asymmetric hurricane wind field as a result of the anticyclonic hurricane winds.

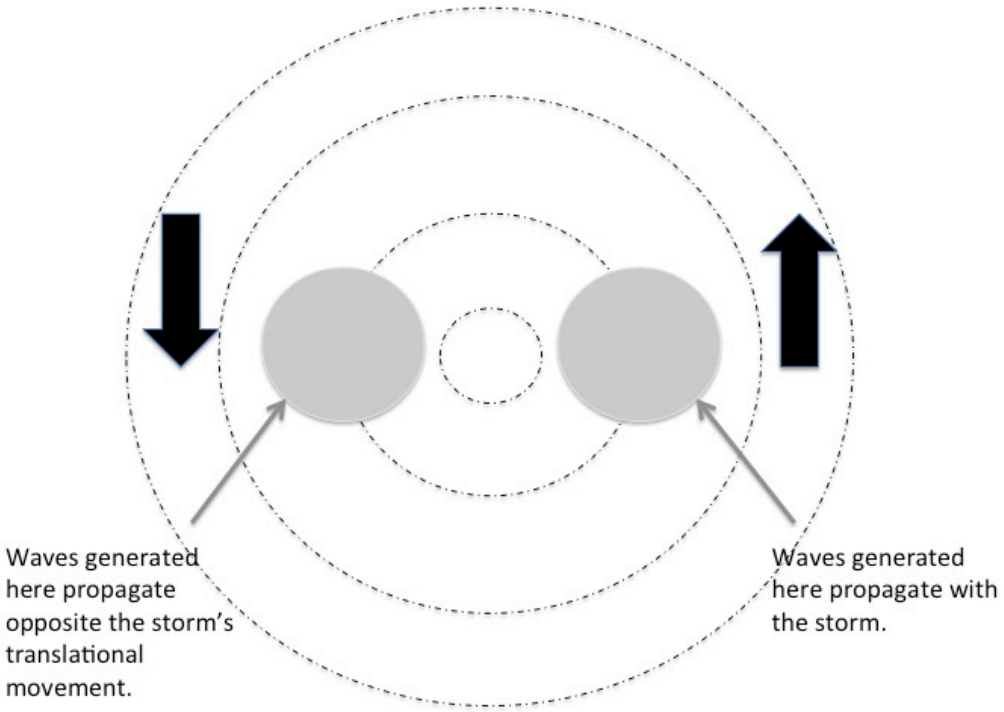

Figure 2.1 Schematic of wave generation within a moving hurricane.

Swell radiates out from the intense region to the right of the storm. The amount of time the wave train spends in the area of intense winds depends on the group velocity of the wave train. Faster wave trains will propagate out from the storm as swell. Wave generated to the left of the storm will propagate in the opposite direction of the storm and subsequently have a much shorter fetch and much lower wave heights (Young 2003). Therefore, it is expected that near shore areas to the far left of the storm will receive smaller wave heights than those closer to the intense wind region to the right of the storm center.

2.1.3 Fully Developed Sea States

Fetch limited water wave growth has been examined in many ocean engineering studies and is vital to limiting wave heights under hurricane conditions. At the fully developed state, dissipation of the wave field due to whitecapping or bottom friction balances the growth of the waves. The JONSWAP (Hasselman et al. 1973) study used data recorded in the North Sea to investigate wind wave growth and was one of the first to quantify growth under fetch-limited conditions. Subsequent studies by Kahma (1981), Kahma and Calkoen (1992) and Walsh et al. (1989) have investigated other aspects of this phenomenon, either by examining new data (Walsh et al 1989) or by rendering existing data into a convenient form (Kahma and Calkoen 1992). However, it was not until Young and Verhagen (1996 a,b,c) that a comprehensive data set for fetch limited wave growth and fully developed conditions for shallow water was developed.

Young and Verhagen developed wind-wave growth curves based upon a set of experiments in Lake George, Australia under ideal conditions. These ideal conditions include a relatively uniform depth (2 meters) across the lake; a long, straight shoreline; and winds unaffected by large obstacles on land (thus providing little disturbance to the atmospheric boundary layer) and traveling over the longest axis of the lake. Although achieving these ideal conditions is impossible, the Lake George experiment provides a reasonable approximation. The desired orientation of winds for wave growth analysis necessitated a long experiment (three years) and significant data filtering to isolate these conditions. They applied power-fitting laws to the recorded data of to develop the following equation:

$$\tilde{H}=\tilde{H}_{\infty}\left[\tanh\left(k_3\tilde{d}\right)\tanh\left\{\frac{k_1\tilde{F}}{\tanh\left(k_3\tilde{d}\right)}\right\}\right]^{q} \tag{2.3}$$

where k_1, m_1, k_3, m_3, and q are coefficients, $\tilde{H}$ is the non-dimensional significant wave height, H_{∞} is the imposed deep-water non-dimensional limit value for significant wave height (Young and Verhagen 1996a), and $\tilde{F}$ is the non-dimensional fetch. H_{∞} is found from the fetch limited growth curves of Pierson and Moskowitz (1964) and determined to be 0.241. Breugem and Holthuijsen (2007) later appended the data set to account for a north-south stratification in the data set. The stratification was due to different wind conditions in the each respective section of the lake and a slight tapering of the southern shoreline. As the fetch approaches a limiting value (based upon the wind speed and depth of the study area), the wave height growth diminishes and a fully developed condition arises. The fully developed state can be observed under large fetch conditions

towards the right hand side of the graph where the curves become constant. In this area wave growth is balanced by different types of dissipation including whitecapping and depth-induced breaking. Breugem and Holthuijsen (2007) formulated this fully developed into a set of growth curves.

These curves and corresponding equations can be used to predict wave heights under fetch limited and fully developed conditions for general scenarios apart from Lake George. Carniello et al. (2012) applied these equations to micro-tidal basins in Venice, Italy. They tuned the curve fitting coefficients of Young and Verhagen (1996a) to fit their test site to minimize error when compared to their dataset.

2.2 Applications of Hurricane Wave Modeling

Simulation of hurricane waves requires the use of wave models such as Simulating Waves Near shore (SWAN) or Steady-State Spectral Wave (STWAVE) coupled to a circulation model such as Advanced Circulation Model (ADCIRC). Coupled ADCIRC-SWAN model validations by Deitrich et al. (2011) have shown the validity of the coupled model. Deitrich et al. (2011) performed hindcasts of Hurricanes Katrina and Rita (2005) and Hurricanes Gustav and Ike (2008). When compared to available measured data for each storm, the coupled ADCIRC-SWAN performed well despite limitations of the input wind fields. Surge R^2 values for ranged from 0.77-0.93 (Dietrich et al. 2011). The H_s showed minimal bias and scatter index (Equation. 4.11-4.12). Hindcast validations of Hurricane Ike were also performed by Hope et al. (2013)

with similar results. However Hope et al. (2013) found that the accuracy of the inland model results was highly sensitive to bottom friction and grid size. This is due to the poor bottom friction parameterization by SWAN and STWAVE for short waves in inland areas. The introduction of the unstructured mesh version of SWAN allowed SWAN and ADCIRC to be run on the same grid and reduced computational limitations while increasing accuracy of the coupled ADCIRC-SWAN model (Dietrich et al. 2010). Coupled ADCIRC-SWAN or ADCIRC-STWAVE have proven to be reliable tools for hurricane hind casts.

2.3 Extreme Value Statistics of Hurricanes

Extreme value analysis involves assessing extreme deviations from the mean of a given probability distribution. Extreme value analysis is most commonly used in hydrology to estimate different flood levels. Numerous studies have examined deep-water wave levels in the Gulf of Mexico (e.g. Panchang et al. 2013, Jonathan and Ewans 2007). These studies have focused on determining extreme event wave heights for use in design of offshore oil and gas facilities. Previous application of extreme value statistics to near shore hurricane waves is limited. However, there has been much discussion in regards to extreme value statistics for surge levels. These methods developed for return period analysis for near shore surge levels could easily be applied to the wave statistics examined in this study. Specifically, the JPM-OS approach first developed by Toro et al. (2010) and Resio et al. (2009). In order to emphasize the

advantage of the JPM-OS, it is important to look at other methods and compare them. Design storm methods were previously used to quantify the 100-year storm in the context of a single event. These methods are currently out of favor because it is impossible to capture all the storm scenarios that cause a surge with yearly 1% chance of occurrence with a single design storm. Historical methods such as high water mark examination and the Empirical Simulation Technique (EST) have long been used to attempt to quantify return periods for coastal flood zones. These methods fail because of the short record of survey and sensitivity to sampling error when extrapolating beyond the record of length (FEMA 2012). The JPM method has become the preferred methodology for analyzing coastal flooding in recent years by it's ability to, in theory, consider all possible storms for a given climatological study area (FEMA 2012). Further discussion of the JPM-OS can be found in Section 5.

2.4 Parameterized Wave Models

There are currently several methods developed for prediction of maximum wave heights during a hurricane event. Typically, these methods have focused on predicting a singular value of wave height (usually the maximum during the event) rather than focusing on the time history or spatial distribution. These models have largely been based on the Bretschneider (1957) concept of equivalent fetch. The equivalent fetch attempts to quantify the complex hurricane wind field and the resulting wave field in terms of a presumed relationship between the maximum wind speed of a storm and the

forward velocity, V_{fm}, of the storm. For a given value of maximum wind velocity V_{max}, the amount of energy transferred to the wave train reaches a maxima when V_{max} and V_{fm} reach an equilibrium, where the waves spend the longest period of time in the area of intense winds to the right of the storm center as explained in Section 2.1.2 (Young 1999). Young (1988) attempts to quantify the equivalent fetch concept based on the results of a numerical wave model (AFDA1) to obtain an empirical representation of equivalent fetch Equation 2.4.

$$X_{eq} = R'\psi[aV_{max}^2 + bV_{max}V_{fm} + cV_{fm}^2 + dV_{max} + eV_{fm} + f], \quad (2.4)$$

Where X_{eq} is the equivalent fetch, V_{max} denotes maximum 10 meter hurricane wind, and V_{fm} is the forward velocity of the storm. The Young (1988) polynomial coefficients determined from curve fitting are $a = -2.175\times10^{-3}$, $b = 1.506\times10^{-2}$, $c = -1.223\times10^{-1}$, $d = 2.190\times10^{-1}$, $e = 6.737\times10^{-1}$, and $f = 7.980\times10^{-1}$. The ψ term is a scaling factor, previously taken as 1 and later defined in Young (2003) as:

$$\psi = -0.015V_{max} + 0.0431V_{fm} + 1.30, \quad (2.5)$$

and the R' term is a spatial scaling parameter related to the storm radius as:

$$R' = 22.5\times10^{-3}\log R - 70.8\times10^{3}, \quad (2.6)$$

where R is the radius to maximum winds. Young (1988) used the equivalent fetch concept in the JONSWAP (Hasselman et al. 1973) fetch-limited wave growth relationship which is expressed as:

$$\frac{gH_s}{U_{10}^2} = 0.0016\left(\frac{gX}{U_{10}^2}\right)^{0.5}, \quad (2.7)$$

where g is the gravitational constant, U_{10} is the 10 m wind speed and X is the fetch

length. Coefficients are derived from deepwater model result simulations. In order to parameterize this relationship to hurricane conditions, Young (1988) proposed replacing the fetch length X with the equivalent fetch X_{eq} in Equation. 2.4. This results in the following parameterization which predicts a single value of H_s^{max} for a given hurricane condition:

$$\frac{gH_s^{max}}{V_{max}^2} = 0.0016\left(\frac{gX_{eq}}{V_{max}^2}\right)^{0.5}, \tag{2.8}$$

Alves et al. (2004) noted that a major limitation of the Young (1988) formulation was that it used a model which incorporated parameterizations for some of the energy propagation terms (referred to as a "second generation" wave model). Alves et al. 2004 modified the Young (1988) parameterization of equivalent fetch by using the results from a third generation wave model (no parameterizations for any of the propagation terms).

While the above equations work well for prediction of wave conditions in deep-water conditions, they are notably lacking for estimation of shallow water waves. A limited water depth affects the propagation characteristics of waves into near shore environments, active wind-wave generation in the near shore, and nonlinear wave-wave interactions and dissipation (Holthuijsen 2007). The United States Army Corps of Engineers, USACE, developed the following shallow water forecasting curves , published in the *Shore Protection Manual* (U.S. Army Coastal Engineering Research Center, 1984) These curves are developed apply methods developed by Bretschneider (1957) fetch limited concept to data from Ijima and Tang (1966) and are as follows:

$$\frac{gH}{U_A^2} = 0.283 \tanh\left(\frac{0.53\bar{d}^{\frac{3}{4}}}{4}\right)\tanh\left[\frac{0.00565\bar{F}^{\frac{1}{2}}}{\tanh\left(0.53\bar{d}^{\frac{3}{4}}\right)}\right], \quad (2.9)$$

where H is the significant wave height, g is the gravitational constant, $U_A^2 = 0.71\ U_{10}^{1.23}$, and $\bar{d}$ is the non-dimensionalized water depth defined as:

$$\bar{d} = \frac{gd}{U_A^2}, \quad (2.10)$$

where d is the depth. The non-dimensionalized fetch term, $\bar{F}$ is defined as:

$$\bar{F} = \frac{gF}{U_A^2}, \quad (2.11)$$

where F is the fetch length. However, these shallow water forecasting curves are not specifically for moving cyclonic storms.

Recently, Taylor (2012) combined these methodologies to examine a spatially dense prediction of H_s^{max} forced by hurricane conditions. Taylor (2012) simulated a suite of ADCIRC-SWAN model results. These results, focused on Corpus Christi, TX were used to formulate the methodology. Taylor (2012) substituted the equivalent fetch calculated using Young (1988), Equation. 2.4, and Alves et al. (2004) relationships for the F term in Equation 2.11. With this modification, maximum significant wave heights for hurricane conditions in finite depth can be determined from Equation. 2.9. Taylor also tuned the coefficients in Equation. 2.8 to minimize error when compared to ADCIRC-SWAN results in bay and open coast locations. The Taylor (2012) methodology will be used as a basis for comparing the effectiveness of the WRF methodology proposed in this thesis.

3. NUMERICAL MODELS AND SITE OVERVIEW

3.1 Model Details

Given the motivation of this study to supplant computationally expensive model runs with parameterizations linking H_s^{max} to hurricane parameters, a sufficient database of previously-calculated model runs must be available for use in parameterization development. An overview of the models used in this study is given in the following sections. It should be mentioned that in order to expedite the development of the WRFs, much of the data was obtained from pre-calculated model runs by outside sources. The use of multiple sources of input data results in the different coupled models used to develop the WRF methodology.

3.1.1 Advanced Circulation Model (ADCIRC)

ADCIRC is a finite element, shallow water model used to resolve water surface elevations from various hurricane conditions. ADCIRC can be run in either three-dimensional or two dimensional depth-integrated forms (Luettich and Westerink 2004). ADCIRC uses either a spherical or Cartesian coordinate system to resolve a finite difference method in time, combined with a finite element scheme in space to solve the Generalized Wave Continuity Equation (GWCE). Both the two- dimensional depth

integrated and three-dimensional versions of ADCIRC solve a vertically integrated form of the GWCE shown in Equation. 3.1 (Luettich and Westerlink 2004):

$$\frac{\partial H}{\partial t} + \frac{\partial}{\partial x}(UH) + \frac{\partial}{\partial y}VH = 0, \tag{3.1}$$

where

$U, V = \int_{-h}^{\zeta} u, v \, dz$ = depth-averaged velocities in the x, y directions,

u, v = vertically-varying velocities in the x, y directions

$H = \varsigma + h$ = total water depth,

h = bathymetric depth,

ς =free-surface surface elevation.

The two-dimensional vertically integrated and three-dimensional versions of ADCIRC substitute vertically integrated momentum equations into the GWCE (Equation. 3.1) to solve for the new free surface elevation (Leuttich and Westerlink 2004). The 2-D non-conservative vertically integrated momentum equations are shown in Equations 3.2 and 3.3:

$$\frac{\partial U}{\partial t} + U\frac{\partial U}{\partial x} + V\frac{\partial U}{\partial y} - fV = -g\frac{\partial\left[\zeta + \frac{P_s}{g\rho_o - \alpha n}\right]}{dx} + \frac{\tau_{sx}}{H\rho_o} - \frac{\tau_{bx}}{H\rho_o} + \frac{M_x}{H} - \frac{D_x}{H} - \frac{B_x}{H} \tag{3.2}$$

$$\frac{\partial V}{\partial t} + U\frac{\partial V}{\partial x} + V\frac{\partial V}{\partial y} - fU$$

$$= -g\frac{\partial\left[\zeta + \frac{P_s}{g\rho_o - \alpha\eta}\right]}{dy} + \frac{\tau_{sy}}{H\rho_o} - \frac{\tau_{by}}{H\rho_o} + \frac{M_y}{H} - \frac{D_y}{H} \qquad (3.3)$$

$$- \frac{B_y}{H}$$

where:

g = gravitational acceleration,

D_x , D_y = momentum dispersion,

M_x , M_y = lateral stress gradient,

B_x , B_y = baroclinic pressure gradient,

f = Coriolis parameter,

ρ_o =water density,

τ_{sx},τ_{sy} =surface stresses,

τ_{bx},τ_{by} =bottom stress components,

P_S = atmospheric pressure,

η= equilibrium tide potential,

α =0.69 (effective Earth elasticity factor).

The dominant physical processes affecting surge output in the two dimensional vertically integrated version of ADCIRC (ADCIRC-2DDI) are the wind surface stresses, baroclinic pressure forcing, currents, bottom stresses, and wave-induced setup (Dean and Dalrymple 2002). The momentum dispersion terms D_x and D_y require knowledge of the vertical profile of horizontal velocity (Leuttich and Westerlink 2004). This is only

possible in the three-dimensional form of ADCIRC; therefore these terms are neglected in ADCIRC-2DDI. Lateral stress gradients M_x, and M_y are also of small significance compared to other terms in the momentum equations (Leuttich and Westerlink 2004). A combination of Equations 3.2 and 3.3 are used to solve for the depth-averaged velocities in the x and y directions, which are then used to solve Equation. 3.1 for the new free-surface water elevation. ADCIRC does not resolve motion on the scale of ocean surface waves, and therefore needs to be coupled to a shallow water wave model in order to determine the effects of wave induced setup on the water surface and to determine the storm induced near shore wave heights. ADCIRC was used in this study coupled to both the SWAN and STWAVE shallow water wave models developed by Booij et al (1999) and USACE (2001), respectively. These models are discussed further in Sections 3.1.2 and 3.1.3.

3.1.2 Simulating Waves Near shore (SWAN)

SWAN is a time-dependent, wave spectral transformation model developed by Delft University of Technology (Booij et al. 1999). The third generation SWAN wave model includes depth-induced breaking and triad wave-wave interactions that are vital for accurate representation of wave conditions in the near shore environment. SWAN uses the action density spectrum, $N(\sigma,\theta)$, in order to be conservative in the presence of near shore currents. The action density spectrum is described in Equation 3.4:

$$\frac{\partial}{\partial t}N + \frac{\partial}{\partial x}c_x N + \frac{\partial}{\partial y}c_y N + \frac{\partial}{\partial \sigma}c_\sigma N + \frac{\partial}{\partial \theta}c_\theta N = \frac{S}{\sigma}, \quad (3.4)$$

where N(σ,θ) is the action density spectrum, S(σ,θ) represents the wave energy sources and sinks, σ is the relative frequency, θ is the wave direction, and c is the propagation velocity of wave action. Examples of wave energy sources include wind inputs, while dissipation is represented by the sum of whitecapping, bottom friction, and depth-induced breaking (Booij et al. 1999). Typically, SWAN is run on a finite-element mesh different from that of ADCIRC. However a version of SWAN has recently been developed that allow execution on unstructured meshes similar to that of ADCIRC, allowing tight coupling of the models for combined hurricane induced surge and wave analysis (Zijlema 2010).

3.1.3 Steady-State Spectral WAVE Model (STWAVE)

STWAVE is a steady state, wave spectral transformation model developed by the U.S. Army Corps of Engineers (USACE 2001). Similar to SWAN, STWAVE is based on the action density spectrum equation shown in Equation. 3.4. Unlike SWAN, STWAVE can only be run as a steady state model, so the first term is not included. A steady state model like STWAVE is useful for wave processes that vary more slowly than the time required for waves to travel through the grid (USACE 2001), as would be the case for a steady state wave field. Complications arise with this assumption when wave generation conditions, such as wind inputs, are rapidly changing, and fetch limited conditions are not attained as a result. This could potentially present problems with

rapidly turning hurricane winds as inputs; however validation of the coupled ADCIRC-STWAVE model with data have shown reasonable accuracy (Zundel et al. 2002).

3.1.4 Planetary Boundary Layer (PBL) Model

Hurricane wind and pressure field forcing used in simulations were generated by the Planetary Boundary Layer (PBL) model developed by Thompson and Cardone (1996). The PBL model uses a moving Cartesian coordinate grid centered at the eye of the storm to solve vertically averaged equations of motion shown in Equations 3.5 and 3.6.

$$\frac{dV}{dt} + f|k \times V| = -\frac{1}{\rho}\nabla p + \nabla \cdot (K_H \nabla V) - \frac{C_D}{h}|V|V \tag{3.5}$$

$$\frac{d}{dt} = \frac{\partial}{\partial t} + V \cdot \nabla \tag{3.6}$$

Where,

V = vertically averaged horizontal velocity,

f = Coriolis parameter,

k = unit vector in the vertical direction,

ρ = air density,

p = atmospheric pressure,

K_H = horizontal eddy viscosity coefficient,

C_D = drag coefficient,

h = height of the PBL.

Hurricane properties are specified at 1 hour intervals along the track, and the PBL model calculates wind and pressure fields at 15 minute intervals. The PBL simulates the hurricane as a steady state snapshot of the hurricane pressure and wind fields. The pressure field is described by Equation 3.7 (Cardone et al. 1994).

$$p(r) = p_o + \Delta p e^{\left(-\frac{R_p}{r}\right)B} \tag{3.7}$$

Where

p_o = central pressure,

Δp = pressure deficit between eye and far field,

R_p = scaling radius,

r = radius,

B = Holland B (Holland 1980) constant in the general range 0.5 – 2.0.

With the hurricane eye as the origin, the PBL model uses a nested grid with linearly increasing spacing as you travel outward from hurricane center. The grid is spaced at 1.25km, 2.5km, 5km, 10km, 20km, 40km, and 80km intervals (Thompson and Cardone 1996). Wind and pressure values are calculated at each node and used as forcing for the coupled ADCIRC-SWAN and ADCIRC-STWAVE models.

3.1.5 Coupling of ADCIRC-SWAN and ADCIRC-STWAVE

As mentioned previously in Section 3.1.1, in order to include the effects of ocean waves on the larger scale hydrodynamics, it is necessary to couple the ADCIRC model

to either SWAN or STWAVE. ADCIRC-SWAN runs simultaneously on the same unstructured mesh, and shares computer resources and forcing mechanisms to provide estimates of both hurricane surge and waves (Dietrich et al. 2010). Water levels and currents are computed via wind inputs to ADCIRC at each node point during the duration of the run. These parameters are passed to SWAN as inputs, along with standard SWAN inputs such as the wind field, to compute all wave related processes and subsequently recalculate the water level as a result of the wave radiation stresses and wave induced setup (Dietrich et al. 2010). Information is passed between models, allowing each to be forced with the information of the other model. The ADCIRC-SWAN model has been used by Dietrich et al. (2010) to hindcast Hurricanes Katrina and Rita with favorable results. Additional model validations using Hurricane Gustav data (Dietrich et al. 2008), surge hindcasts near the Mississippi River delta (Martyr et al. 2013), and various Gulf of Mexico hindcasts (Dietrich et al 2012) have demonstrated the effectiveness of the coupled ADCIRC-SWAN model.

ADCIRC-STWAVE coupling works similarly to ADCIRC-SWAN, with differences resulting from the selected wave model mentioned in Section 3.1.3. ADCIRC-STWAVE coupling is achieved via the Coastal STORM Modeling-System (CSTORM-MS) developed by the USACE. Two-way "steering" of the models is accomplished via the Surface-Water Modeling Systems (SMS) Steering Module, where current and wave data are shared between the models (Zundel et al. 2002). Deepwater waves are calculated via the WAve prediction Model (WAM), until the storm reaches the finer STWAVE mesh boundary near the coast. Both WAM and STWAVE run on

structured grids, requiring interpolation from the ADCIRC unstructured grid to achieve model coupling. ADCIRC-STWAVE simulations are generally more expedient than ADCIRC-SWAN runs due to the exclusion of the time dependent term in the action balance spectrum governing equation (Equation. 3.4).

3.2 Simulation Area

Three coastal communities along the Gulf of Mexico were selected for this combined wave and surge study: Corpus Christi, Texas; Gulfport, Mississippi; and Panama City, Florida. Each city provides a unique environment in which to study the physics of wave parameterization and conduct eventual damage effects on the surrounding industry and community. A map of all three cities is shown in Figure 3.1. Previous wave and surge analysis were conducted by Udoh (2012) and Taylor (2012) at Corpus Christi, Texas.

According to the US Census Bureau, 19 million people live within 80km of the Gulf of Mexico shoreline, with 86 people per square kilometer (US Census 2010). This population density is roughly three times the national average. With such a densely populated area, it is important to quantify key features that may affect wave generation off the coast of each city, as well as potential infrastructure damages that may occur from surge inundation and repeated battering from wave-structure interaction.

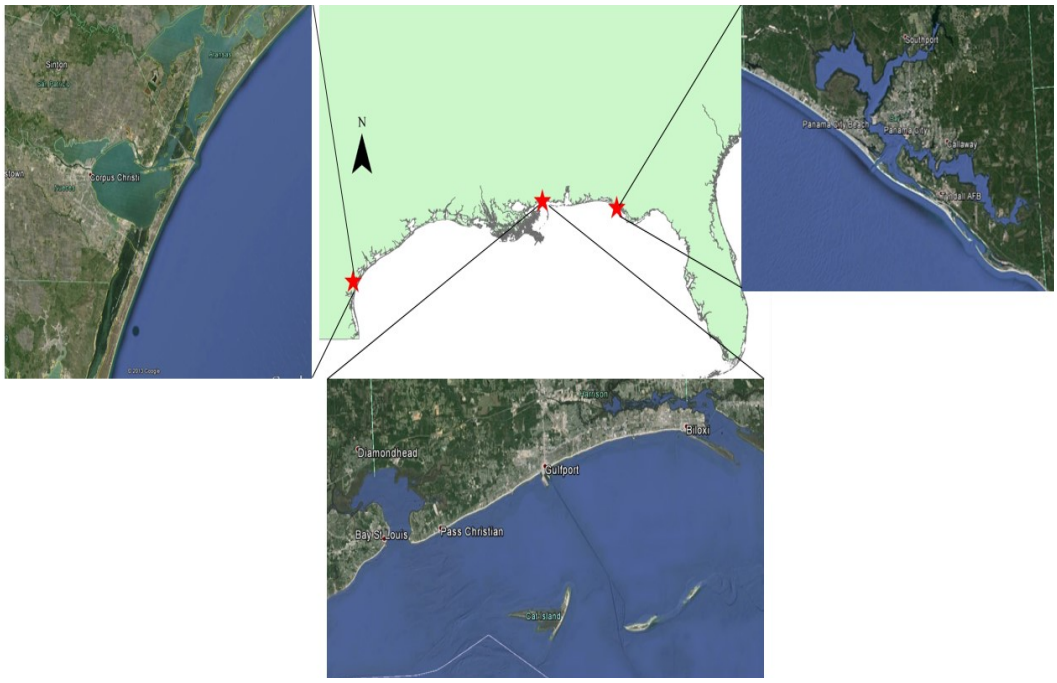

Figure 2.1 Location of the three study sites along the Gulf Coast as well as enlarged satellite photos of each site. Site name counter-clockwise from upper left: Corpus Christi, TX, Gulfport, MS, Panama City, FL.

Corpus Christi, TX is a coastal community located in southeastern Texas. The city is separated from the Gulf by a 2.5 km wide barrier island and Corpus Christi Bay. Home to 305,000 residents (2010 U.S. Census Bureau), Corpus Christi relies heavily on tourism and is home to multiple oil refineries. Hurricane Bret and Hurricane Allen affected both Corpus Christi. In 1980, Hurricane Allen caused an estimate $300 million in total damages, with much of the destruction concentrated in the Corps Christi area (Lawrence and Pelissier 1981). Corpus Christi provides a unique environment to test and develop the WRF methodology for bay locations located behind a barrier island system. Overtopping of the barrier island will cause much of the wave energy seen along the open coast to dissipate, allowing wave re-generation across the bay along a much shorter fetch. As a result of the limited exposure to open ocean conditions, wave heights in bay locations are expected to be smaller than those on the open coastline. A map of all 159 WRF analysis stations is shown in Figure 3.2. Overtopping, which is the complete inundation of a section of barrier island, and its effects on wave generation are implicitly included in the WRF methodology, since the results of the coupled wave-surge models used to generate the WRF include overtopping. Open Coast locations are directly exposed to the open sea, and therefore ocean surge; higher wave heights are thus expected at these locations. Extreme value application of the WRF method can be used to estimate damage vulnerability due to extreme wave events, which will aid in both economic and social planning.

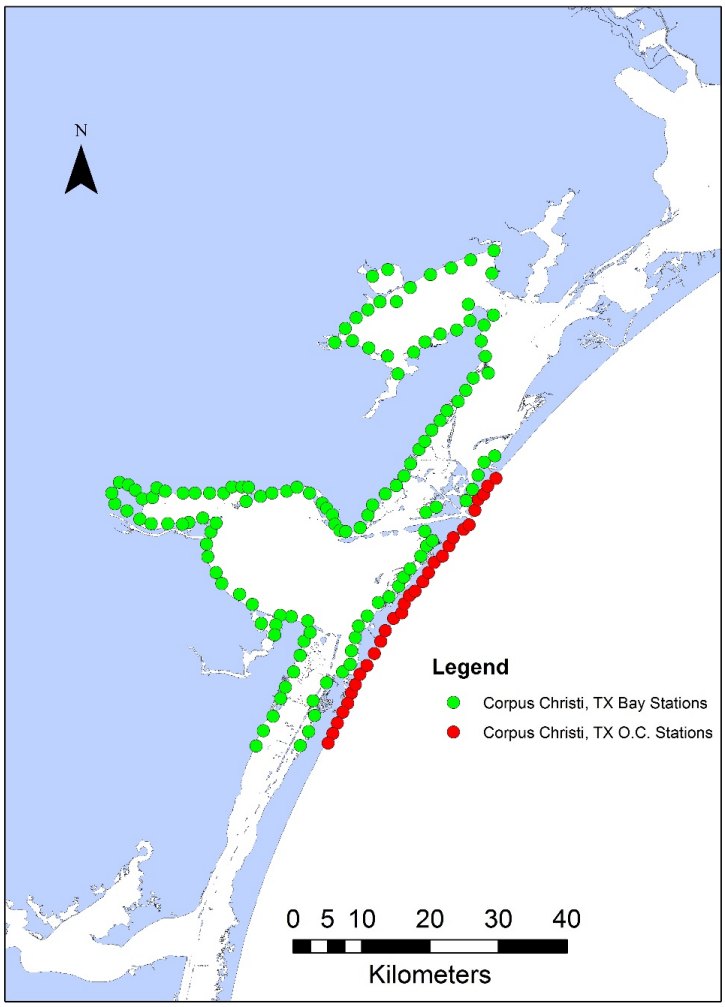

Figure 3.2 WRF Station locations for Corpus Christi, TX. All 159 stations shown, with 30 bay stations and 129 bay stations delineated by color

Gulfport, MS is the second largest city in MS and is home to 68,000 residents (US Census Bureau 2010). The Port of Gulfport, located near city center along the waterfront, ships more than 2 million tons of cargo annually. The city has been affected by recent hurricanes including Elana in 1985 and Katrina in 2005. Gulfport provides a unique environment to test the WRF methodology due to the nearby Mississippi delta and numerous near shore islands, including Ship, Cat and Horn Islands. Bay stations located in Bay of Saint Louis to the west and Biloxi Bay to the east also provide two unique environments to tune the bay WRF methodology. A map showing all 165 WRF stations is shown in Figure 3.2. The Bay of Saint Louis is extremely shallow (average depth < 1 m) and large portions are exposed to the open coast via the inlet separating Bay of St. Louis, MS from Gulfport, MS. Larger wave heights are expected at stations exposed to open coast forcing via the inlet, with smaller wave heights expected at sheltered stations in the bays marshy east and west corners. Biloxi Bay is more sheltered from open sea forcing mechanisms via Deer Island, and its long, fingerlike structure with numerous islands is expected to minimize wave heights at the back bay stations.

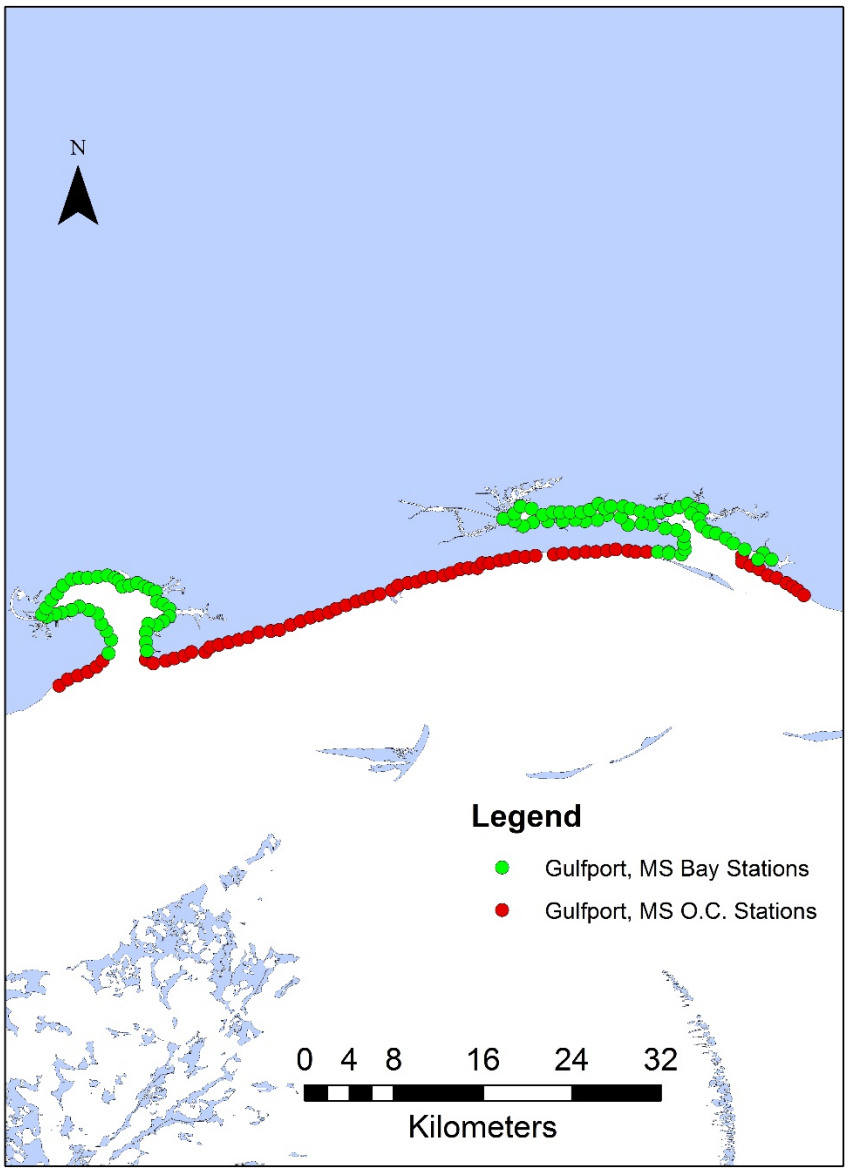

Figure 3.3 WRF Station location and map of surrounding area for Gulfport, MS. 70 O.C. stations shown in red and 95 Bay stations shown in green. Note: Bay of St. Louis located on Western side of map, while Biloxi Bay is to the East.

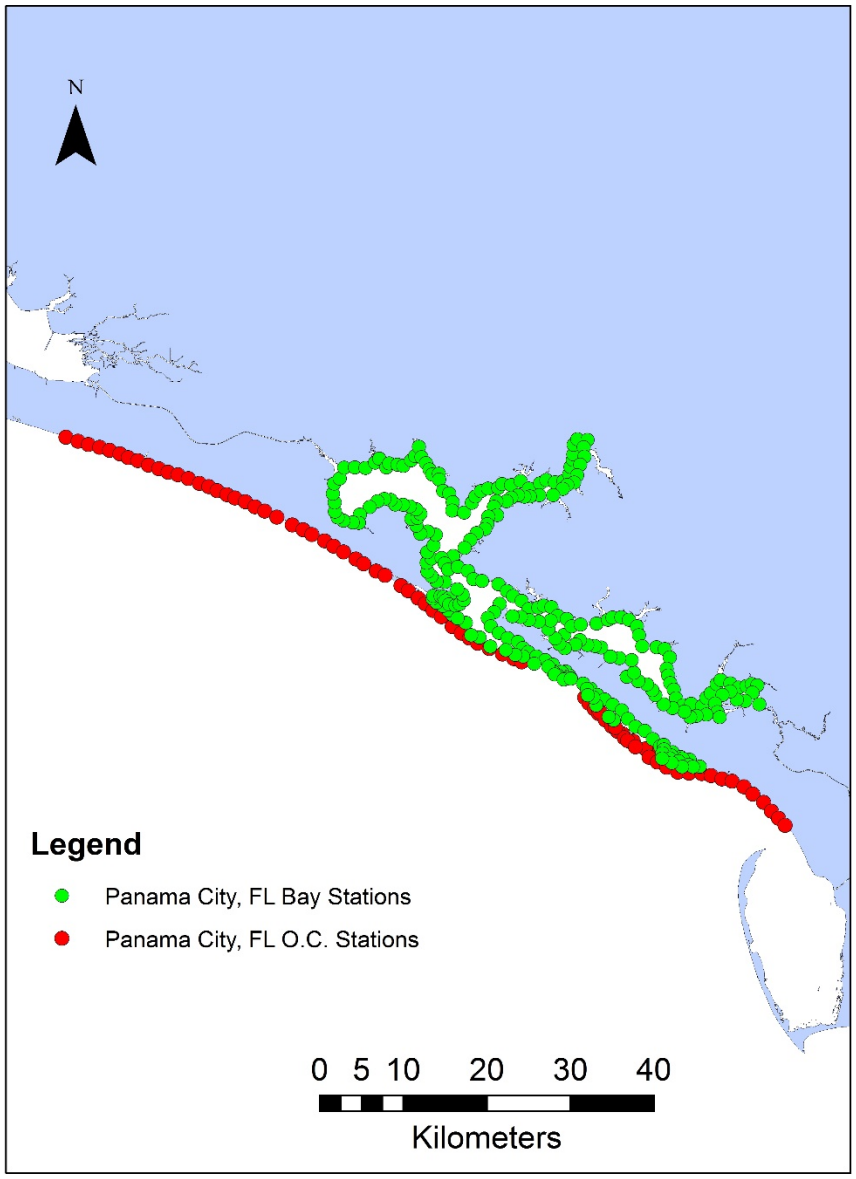

Figure 3.4 All 346 WRF stations shown for Panama City, FL. 74 Open Coast stations shown in red and 272 bay stations shown in green.

Currently home to 36,000 residents (2010 U.S. Census Bureau), Panama City, FL is located on the Florida panhandle between Tallahassee and Pensacola. Panama City was included in this study for its wealth of previous data, and to investigate the effects of wave damage on a residential coastal town without major port facilities. Panama City has suffered substantial Hurricane damage from Ivan (2004) and Eloise (1975). In 1975 Eloise caused four deaths and an estimated property loss of 200 million dollars (NOAA 1975). Near shore wave heights during Eloise reached roughly 8 m along the Panama City shoreline. The Panama City, FL open coast shoreline faces southwest, allowing for the investigation of the WRF methods effectiveness with a differently oriented shoreline. All 346 WRF stations are shown in Figure 3.4. The bay stations in Panama City allow examination of the effects of a complicated bay system with a relatively narrow inlet, combined with a short barrier island spanning the western edge of the bay systems mouth.

4. WAVE RESPONSE FUNCTION DEVELOPMENT AND ANLALYSIS

4.1 Introduction to Development

This section presents the formulation and analysis of physics based hurricane wave response functions. In Sections 4.1.2 the selection of key parameters for non-dimensional functions is discussed. The selection of these parameters will use available data and existing literature to determine the best non-dimensional parameterization of hurricane wave heights. In Section 4.1.3 we discuss the need for refinement of this strategy and application of a fully developed sea state cap in combination with the non-dimensional equations discussed in Section 4.1.2. Details of the application of the WRF method to bay stations at all three test sites is outlined in Section 4.1.4, while the application of the WRF method to open coast stations is shown in Section 4.1.5. Section 4.1.6 provides conclusions for the WRF methodology. Section 4.2 compares the WRF methodology to existing hurricane wave prediction methods developed by Taylor (2012) and performs a validation with data from Kennedy et al. (2011). Finally, Section 4.3 presents the conclusions of the H_s^{max} parameterization results.

4.1.1 Parameter Selection

To to accurately create a parametric description of H_s^{max} in the form of non-dimensional equations, it is first critical to select the most important physical properties

of a hurricane, which control near-shore wave growth. Parameters specifying the critical physical properties investigated in this study include track location, landfall position, minimum distance to storm track, central pressure, radius to maximum winds, translational speed, surge depth, bathymetric depth, and wind speed. Proper arrangement of these equations in non-dimensional form will collapse the data so curve fitting methods can be applied and unique best fit equations developed at each station. Each curve fitting procedure considered linear, second- order polynomial, and power law fits. Back prediction of storms entails using the WRF method to predict H_s^{max} from given storm parameters, and compare to model results. An optimal fit would minimize Root Mean Square Error (RMSE) in back prediction of H_s^{max} when compared to the data from which these were derived.

Sensitivity analysis conducted by Taylor (2012) detailed the response of hurricane waves to changes in many of these parameters. Taylor's analysis involved simulation of different hurricanes via the coupled ADCIRC-SWAN model and analysis of wave height time series at near-shore locations. His analysis investigated sensitivity to landfall location, central pressure, translational speed, and radius to maximum winds. Taylor found that the point of landfall relative to station under consideration is vital because of the counterclockwise winds which cause an uneven distribution of wave heights (Young 2003). Storms making landfall to the left (West) of the point of interest generated maximum wave heights that were 29.3% higher at the shoreline and 55.6% higher in the bay than storms that made landfall to the right (East) of the point of interest (Taylor 2012). These findings illustrate the need to consider landfall position in the

WRF formulation. Taylor's analysis of the effect of central pressure showed that with increasing pressure deficit, higher waves were generated at shoreline and bay locations. Taylor's analysis of radius to maximum winds yielded similar results, with increased storm size resulting in larger wave heights in the near-shore area. Translational speed has a greater effect on hurricane surge than hurricane wave heights. Slower moving storms have a longer time to build up storm surge (Udoh 2013). Since wave generation in the near-shore environment is such a depth dependent process, surge depth can be included in the non-dimensional formulation instead of directly considering translational speed.

Based upon the findings of Taylor (2012) and accepted dynamical principles of wave generation and evolution in shallow water (Holthuijsen 2007, Dean and Dalrymple 2002) the following parameters were selected for development of the non-dimensional WRF formulation:

- radius to maximum winds R,
- central pressure deficit ΔC_p,
- d_s storm depth (surge depth +bathymetric depth),
- and minimum distance to the storm track D_{min}.

The minimum distance to the storm track was chosen under the assumption that the maximum wave height will occur when the distance from station under consideration to storm center is minimized. This assumption is made due to the presumed maximum wind speed occurring at this point.

To validate the assumption of coincidence between maximum wave height and minimum distance to storm track, the time series of maximum wave heights for selected ADCIRC-SWAN storms simulated at Gulfport, MS were analyzed. Time series analysis of a midrange storm was performed at all 165 stations in Gulfport, MS. Time series of surge levels and significant wave heights, H_s, were extracted at all stations from coupled ADCIRC-SWAN output files. The two goals of time series analysis were: (1) compare time of occurrence of maximum H_s and surge, and (2) determine if H_s^{max} values occurred at minimum distance to storm track. If the peaks of surge and wave height are concurrent, then using maximum surge as an input into the non-dimensional WRF's would be an accurate characterization of actual physical storm conditions. Time series plots of open coast station #47, as well as bay stations # 25 (located in Bay of St. Louis) and bay station #125 (located in Biloxi Bay) are shown in Figures 4.1 and 4.2, respectively.

Analysis of the time series at all 165 stations yielded similar results to those shown in Figure 4.1 and Figure 4.2. Mean absolute difference between the times of occurrence of peak surge and maximum wave height over all stations was 1.067 hours. In addition, the mean absolute and percentage differences between the maximum wave height, and the wave height at the time of maximum surge, were -0.10m and 5%, respectively. This is due to the slight lag (around 1 hour) between maximum surge event and maximum wave event. This minimal difference indicates that using the peak surge as an input into the non-dimensional WRFs is a valid assumption that will introduce nominal physical error into the equations. It should also be noted that in future JPM

analysis, maximum surge will be predicted and used as an input to determine extreme value statistics for waves. Any error introduced by the WRF method can be included in the JPM-OS analysis as uncertainty.

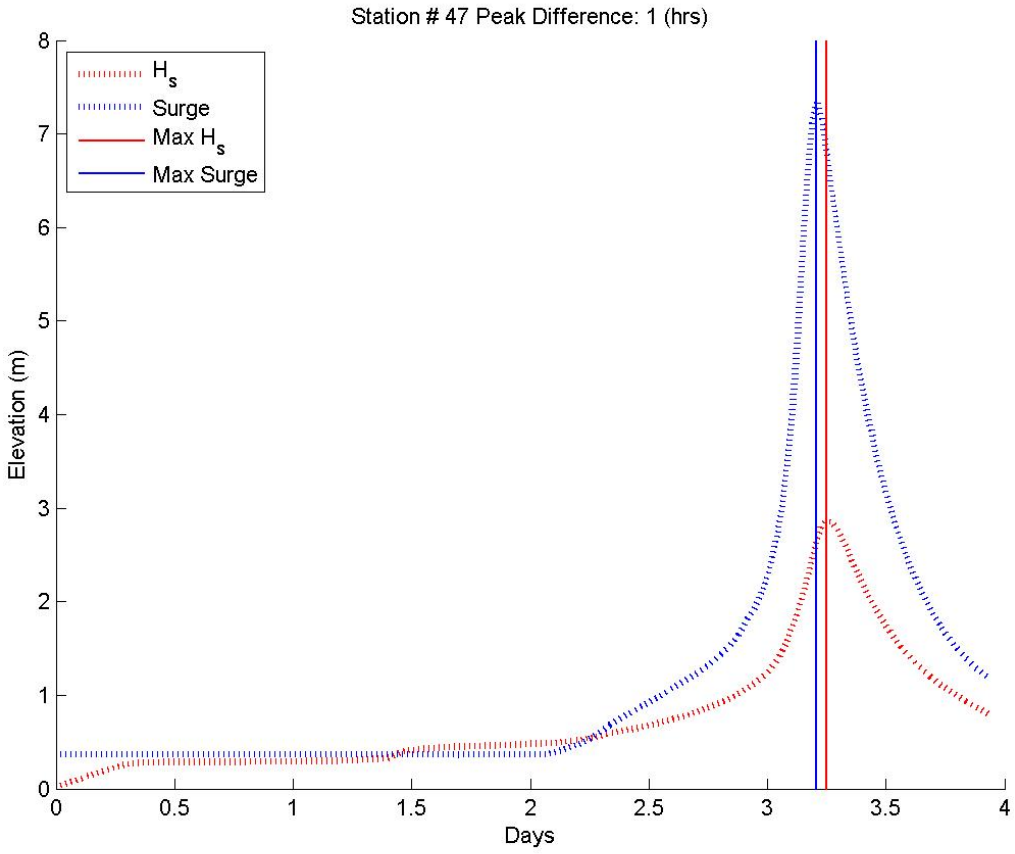

Figure 4.1 Time series for Open Coast station #47. Note that maximum wave event (vertical red line) occurs 1 hour after maximum surge event (vertical blue line). X-axis shows days since start of simulation. Y-axis shows elevation of given event.

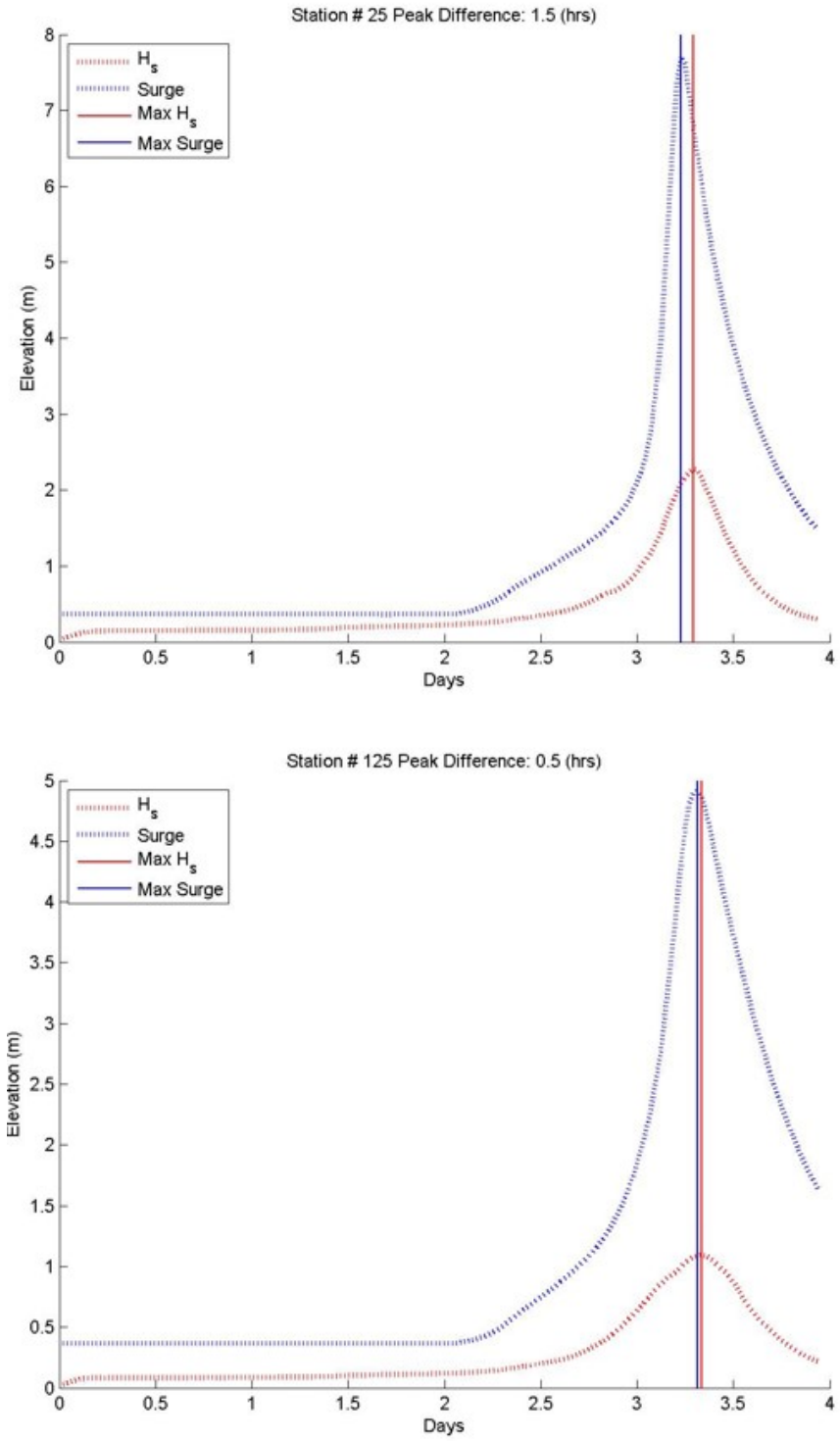

Figure 4.2 Time series for: Top- Bay station #25 (Bay of St. Louis), and Bottom- Bay station #125 (Biloxi Bay). Maximum wave events (vertical red line) occur after maximum surge events(vertical blue line) for both stations. X-axis shows days since start of simulation. Y-axis shows elevation of given event.

If the minimum distance to storm track is to be used in the non-dimensional formulation, H_s^{max} should occur near or at this distance. The difference between the time of occurrence of H_s^{max} and D_{min} was calculated based upon the time series plots shown in Figures 4.1-4.2 and storm track information used as input into the PBL model. First, the time since the start of the storm genesis was calculated for D_{min} and H_s^{max}. This was done for all 165 stations. Mean difference between the time of H_s^{max} and D_{min} was only 13.8 minutes. The close temporal spacing of these two events indicates that using D_{min} as an input parameter into the non-dimensional formulation will introduce minimal error when back predicting H_s^{max}.

Different arrangements of the chosen hurricane parameters were investigated until a superior option emerged. To ease computational burden and in hopes of developing a more universally applicable methodology, a singular arrangement of the non-dimensional parameters was chosen. This greatly simplified analysis when the JPM-OS methodology was applied. The final non-dimensional formulation can be seen in Equation 4.1.

$$\frac{H_{s\,max}R}{D_{min}d_s} = \sqrt{\frac{\Delta C_p R}{D_{min}d_s}}, \tag{4.1}$$

The arrangement, including repeating variables on each side of the equation, is similar to that of Young's (1988) modification to the Hasselmann et al. (1980) fetch limited wave growth relationship Equation. 2.8. Equation. 4.1 was used to parameterize wave heights for each station, at each location.

Curve fitting was done to represent the effect of landfall position on wave growth; however, due to the east-west asymmetry of the wind structure in the hurricane, a further grouping of storms based on position relative to landfall was performed. Storms that make landfall to the right (East) of the suite of WRF stations were grouped together for curve fitting. Due to the anti-cyclonic nature of hurricane winds, waves in this region spend longer traveling with the storm in the region of intense winds and as a result higher wave heights are expected (Young 2003, Taylor 2012). The opposite is true for storms that make landfall to the left (West) of the suite of WRF points. This group of storms are fit together as well. Finally, storms that make landfall within the range of WRF stations are fit together as a group. This third category was done to avoid grouping storms that narrowly miss a selected point (either to the left or right) with storms that make landfall farther away, where the station is subject to vastly different wave generation mechanisms. Figure 4.3 shows an example of a sample station and the storms which will be grouped into the different fitting categories. Note that the example curve fittings are all open coast stations. Examination of overall accuracy of the non-dimensional method and examination of results in bay stations occurs in Section 4.1.2.

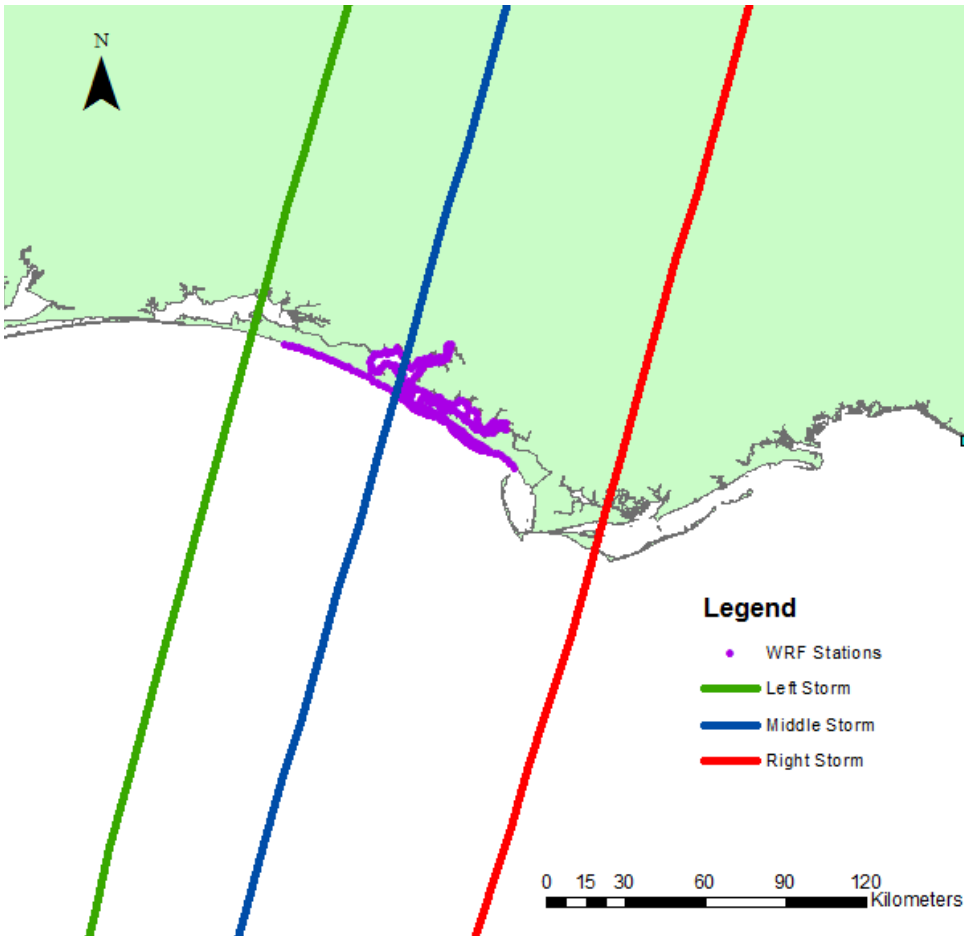

Figure 4.3 Example of different categories of storms for each type of fitting. Left, Middle, and Right storms grouped together. Example storm tracks shown for each category of storm at Panama City, FL.

The type of fit will be chosen to minimize RMSE when compared to ADCIRC-SWAN or ADCIRC-STWAVE model results. An example of the curve fitting methods applied to each study site is shown in Figure 4.4.

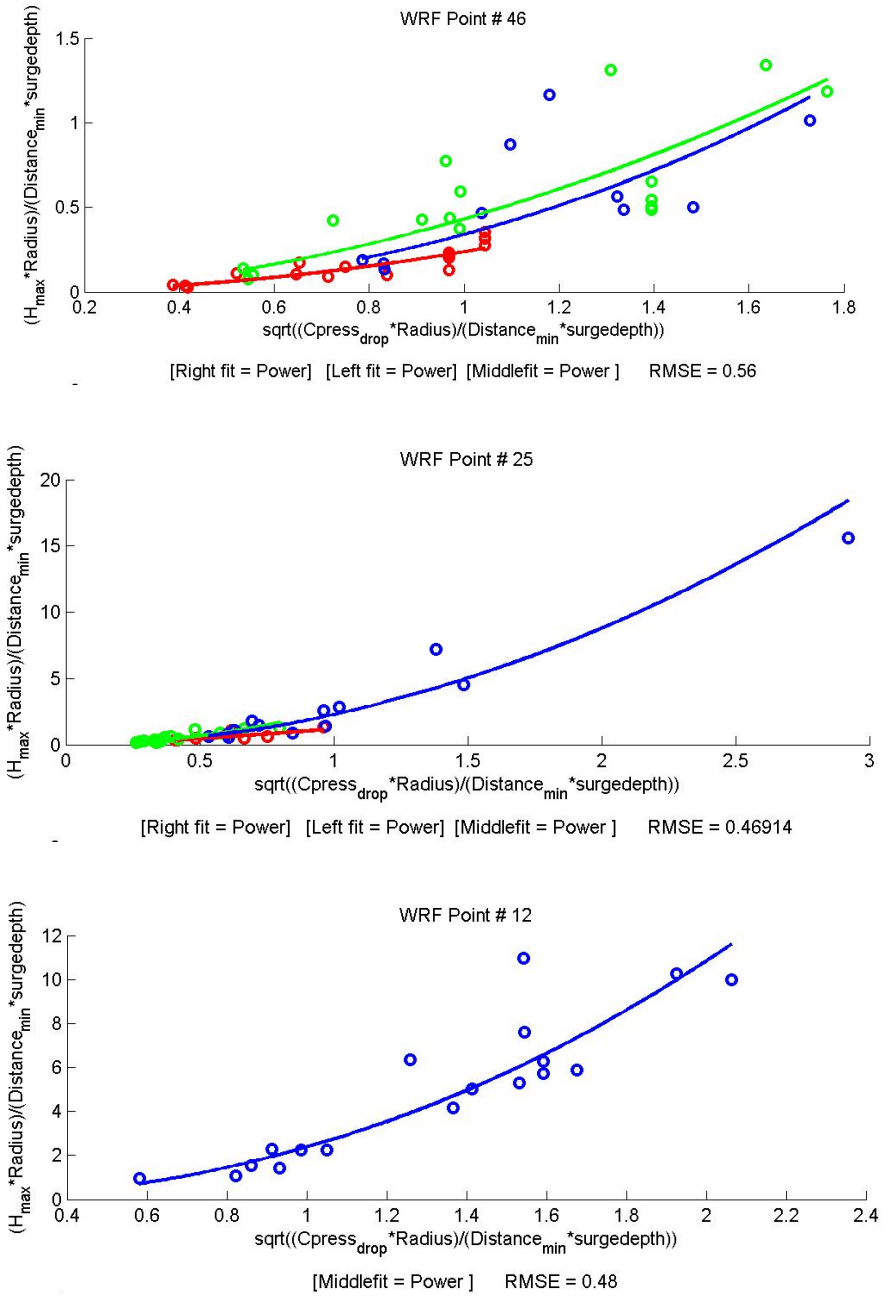

Figure 4.4 Fitting examples for all three test sites. Site Names from top to bottom: Gulfport, MS, Panama City, FL, Corpus Christi, TX. Red lines represent storms making landfall to the right, green to the left, and blue in the middle of the suit of WRF points. For reference, fitting colors correspond to example storms in Figure. 4.1

4.1.2 Application of the Non-dimensional Formulation

Equation 4.1 was applied to all stations at all three test locations. Curve fitting was performed as described in Section 4.1.2. Once curve fitting equations are developed based on Equation 4.1, H_s^{max} can be back predicted and compared to the ADCIRC-STWAVE or ADCIRC-SWAN model results. Examples of the 2nd order polynomial, power law, and linear curve fits are seen in Equations 4.2-4.4 respectively,

$$H_s^{max} = \frac{\left[\left(ax'^2 + bx' + c\right)D_{min}d_s\right]}{R}, \tag{4.2}$$

$$H_s^{max} = \frac{\left[\left(dx'^e\right)D_{min}d_s\right]}{R} \tag{4.3}$$

$$H_s^{max} = \frac{\left[(fx' + g)D_{min}d_s\right]}{R} \tag{4.4}$$

where *a-g* are curve fitting coefficients unique to each station, and *x'* is equal to the RHS of Equation.4.1. By using these equations, values of H_s^{max} can quickly be found at each station in a computationally efficient manner.

Application of curve fitting equations 4.2-4.4 to both open coast and bay stations yielded mixed results. RMSEs and Normalized Root Mean Square Errors, NRSME, (Equation. 4.5) were calculated at each station by comparing WRF results to model results.

$$NRMSE = \frac{RMSE}{x_{max} - x_{min}}, \tag{4.5}$$

Where x_{max} and x_{min} are the maximum and minimum H_s^{max} at each station throughout all simulated storms. Tables 4.1 and 4.2 show minimum, maximum, and mean RMSE's as well as NRMSE's at bay and open coast stations for all locations.

Table 4.1 RMSE's at all bay stations.

Location	Minimum (m)	Maximum (m)	Mean (m)	NRMSE (%)
Gulfport, MS	0.082	0.63	0.25	17.5
Panama City, FL	0.06	0.43	0.21	21.3
Corpus Christi, TX	0.16	0.66	0.32	25.5

Table 4.2 RMSE's at all open coast stations

Location	Minimum (m)	Maximum (m)	Mean (m)	NRMSE (%)
Gulfport, MS	0.38	0.82	0.53	14.5
Panama City, FL	0.21	0.61	0.33	19.5
Corpus Christi, TX	0.15	1.4	0.40	22.8

Large RMSEs at open coast locations can likely be attributed to larger wave heights reaching these locations. However the much large NRMSEs, which take into account the range of wave heights seen at a given station, indicate that the WRF methodology must be adjusted at all locations. Higher wave heights are consistently over-predicted at open coast locations, as well as many bay locations. Figure 4.5 shows back prediction at Gulfport, MS open coast station #47 and bay station #25. Notice the

over-prediction of larger wave heights at both stations in Figure 4.5. These over-predictions are seen at many stations.

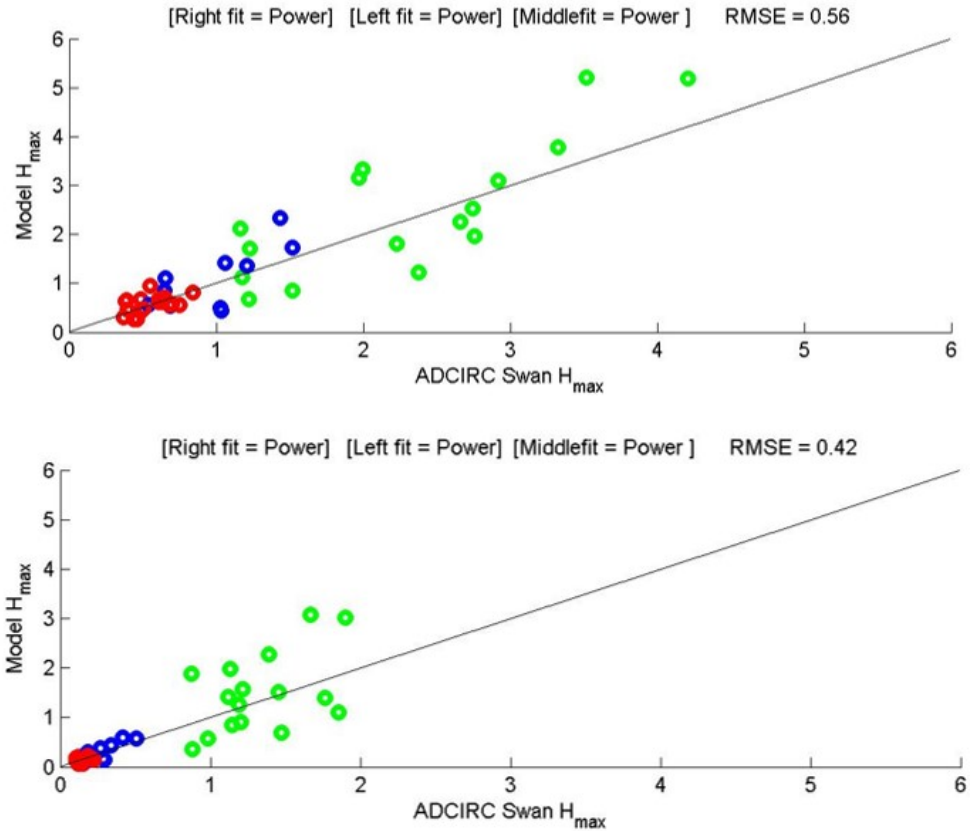

Figure 4.5 Back Prediction at open coast station # 47 (Top) and bay station #25 (bottom). Color coding as follows: Green- storms that make landfall to the left (West) of the WRF points; Blue- storms that make landfall in the middle of the WRF points; Red- storms that make landfall to the right (East) of the WRF points.

The over-prediction of higher wave heights occur mainly with storms that make landfall to the left (West) of the suite of WRF stations. These storms typically produce the highest wave heights, so it is important that their H_s^{max} values be properly quantified

in order to perform accurate extreme value analysis. In the following section we introduce an upper limit to wave height based on the concept of a "fully-developed sea," in which the generation of wave energy by wind is balanced by the dissipation due to whitecapping, depth-limited breaking, and bottom friction. Formulations which describe this fully-developed condition will be used in combination with the non-dimensional WRF's to limit the over prediction seen in Figure 4.5 and Tables 4.1-.

4.1.3 Addition of a Fully-Developed Sea State Cap to Methodology

It is apparent from the back prediction graphs shown in Figure 4.5 and discussion of Section 4.1.2 that solely using the non-dimensional equations, as the WRF methodology will not accurately parameterize hurricane wave heights. Open Coast locations are especially poorly represented by Equations 4.1-4.4. Open Coast stations are often subject to the highest wave heights, so it is extremely important to accurately predict wave heights at these stations.

Under constant wind speed and direction it is well known that shallow water wave heights reach a limiting value (Holthuijsen 2007). The conditions which lead to this limiting value of wave height is called a fully developed sea state and is detailed fully in Section 2.1.3. Although hurricane winds are not constant in speed and direction, near-shore waves can still reach a fully developed state where growth is limited and dissipation is maximized (Ochi 2003). Shallow water, fetch limited growth equations (Equation. 2.3) developed by Verhagen and Young (1996) and later revised by Breugem

and Holthuijsen (2007) are used for development of a fully developed sea state under hurricane conditions that can be adjusted for each station. The curves flatten out under fully developed, non-fetch-limited conditions, and show virtually no dependence of wave height on wind speed above a particular value. In order to provide a "cap" on wave height predictions and prevent wave growth beyond this fetch limited condition, Equation. 4.6, based on Breugem and Holthuijsen (2007) is used. Equation. 4.6 eliminates the fetch term in order to approximate the flat, fully developed portion of the curves .The fully developed sea state equation that will be used as a limiting cap on wave heights predicted by equations 4.1-4.4 is shown below:

$$\widetilde{H} = \widetilde{H}_{\infty}\left[\tanh\left(a_1 \tilde{d}^{b_1}\right)\right]^{c}, \tag{4.6}$$

where:

$a_1, b_1, c_1 =$ constants optimized at each location to minimize RMSE when compared to model results,

and

$$\tilde{d} = \frac{gd}{U_{10}^2}, \tag{4.7}$$

$$\widetilde{H} = \frac{gH_s}{U_{10}^2}, \tag{4.8}$$

where

$d =$ total water depth.

These equations require coefficient optimization at each station. . This optimization follows the procedure of Carniello et al. (2011), who tuned the Verhagen and Young (1996) data set coefficients to model short wind-waves in micro-tidal basins. Coefficients are adjusted until RMSE is at a minimum.

One issue that arises with using a fully developed sea state as a cap on wave height growth is the need for U_{10} as an input. An accurate prediction of 10 meter wind speed is essential in valid predictions of the fully developed wave height found in Equation. 4.6-4.8. Rather than use a computationally-intensive PBL (or similar) model, the Holland (1980) hurricane wind parameterization was used to calculate U_{10}. In order to obtain the maximum wave height under fully developed conditions, it is essential to find the maximum wind speed each point experiences during the course of the storm.

Based on the time series analysis in Section 4.1.1, it is apparent that the maximum wave conditions are nearly concurrent with the minimum distance to storm track D_{min} being at a minimum; this is assumed to correspond to the time of maximum wind speed at the station of interest. To predict the maximum wind speed at each station over the course of a given hurricane event, Equation 4.9 (from Holland 1980) is used to predict the wind speed at each WRF station outside of the radius to maximum winds.

$$U_{max} = \left[\frac{AB(p_n - p_c)\exp\left(-\frac{A}{r^B}\right)}{\rho r^B} + \frac{r^2 f^2}{4}\right]^{0.5} - r\frac{f}{2} \tag{4.9}$$

Where U_{max} is the maximum 10 m wind speed at each station during the course of the storm, B is a scaling parameter describing the spatial distribution of the wind field, $A = R^B$ (where R is the radius to maximum winds in the hurricane) ρ_n is the ambient

atmospheric pressure (in millibars), ρ_c is the central pressure (also in millibars), r is the radial distance to storm (taken as D_{min}), and f is the Coriolis parameter. The distance to storm track is used as r to predict U_{max} at each WRF station located outside of the radius to maximum winds (R). At distances near R, the Coriolis terms are neglected because they are small in comparison to the pressure gradient (Holland 1980). If D_{min} was used to predict U_{max} at these stations, the maximum wind speed would be greatly under predicted. Instead, U_{max} at these stations is calculated when the radial distance is equal to the radius to maximum winds as seen in Equation 4.10.

$$U_{max} = \left[\frac{AB(p_n - p_c)\exp\left(-\frac{A}{R^B}\right)}{\rho * R^B}\right]^{0.5}, \tag{4.10}$$

Once the coefficients are tuned to each station and U_{max} is predicted, Equations 4.6-4.8 can be used in combination with Equation. 4.1.-4.4 to best predict maximum wave heights at open coast and bay locations for a given storm. The functionality of using these two sets of equations as the full Wave Response Function method is as follows:

1. Predict H_s^{max} based on the non-dimensional formulation from Equation. 4.1-4.4
2. Predict U_{max} experienced during the course of the storm at each station from Equation. 4.9-4.10.
3. Predict H_s^{max} from equations 4.6-4.8 using U_{max} predicted in step 2.

Using the three steps above, the bay and open coast methodology will be described in the following sections.

4.1.4 Bay Station WRF Methodology and Application

In bay locations, the maximum significant wave height predicted from the non-dimensional curve fitting equations (Equation 4.1-4.4) is used in combination with the fully developed wave height predicted from Equations 4.6-4.8. The maximum wave heights at bay stations may not be adequately described by the fully-developed sea formulations. In many instances, the water depth may be too shallow, or the fetch too short, to be within the range of the conditions for which Equations 4.6-4.8 were derived. To correct this difficulty, a combination of non-dimensional (equation numbers) and fully developed equations (equation numbers) is employed. The complete WRF methodology used in bays is:

1. Predict H_s^{max} based on the non-dimensional formulation from Equation. 4.1-4.4
2. Predict U_{max} experienced during the course of the storm at each station from Equation. 4.9-4.10.
3. Predict H_s^{max} from fully developed equations 4.6-4.8 using U_{max} predicted in step 2.
4. If (1) is greater than (3) the non-dimensional equations are over predicting the wave height, a fully developed condition is assumed, and (3) is taken as the final wave height.
5. If (1) is less than (3), it is assumed that a fully developed condition has not yet been attained, and (1) is taken as the final maximum significant wave height.

Verification of the bay station methodology was done through RMSE comparisons for two different methods. The methods investigated are as follows:

1. H_s^{max} predicted solely based on the non-dimensional equations.
2. H_s^{max} predicted using the combined methodology described earlier in this section.

Using the fully developed equations alone was not considered. Comparison of the two methods is seen in Table 4.3. It is apparent that sole use of the non-dimensional equations in bay locations introduced substantially more error than the combined methodology.

Table 4.3 RMSE's averaged across all bay stations for Non-dimensional and Combined methods described above.

Location	Non-dimensional	Combined
Corpus Christi, TX	0.31	0.22
Gulfport, MS	0.25	0.21
Panama City, FL	0.21	0.19

Figure 4.6 shows an example of the wave heights predicted from the non-dimensional and fully developed methods, compared to the ADCIRC-STWAVE model results for all 45 storms simulated at bay station #20 in Gulfport, MS.

Here storms 34-37 are especially over predicted by the non-dimensional equations. These storms are intense (low central pressure) storms that produce larger wave heights. This illustrates the need for the combined use of the fully developed and non-dimensional equations in the WRF methodology.

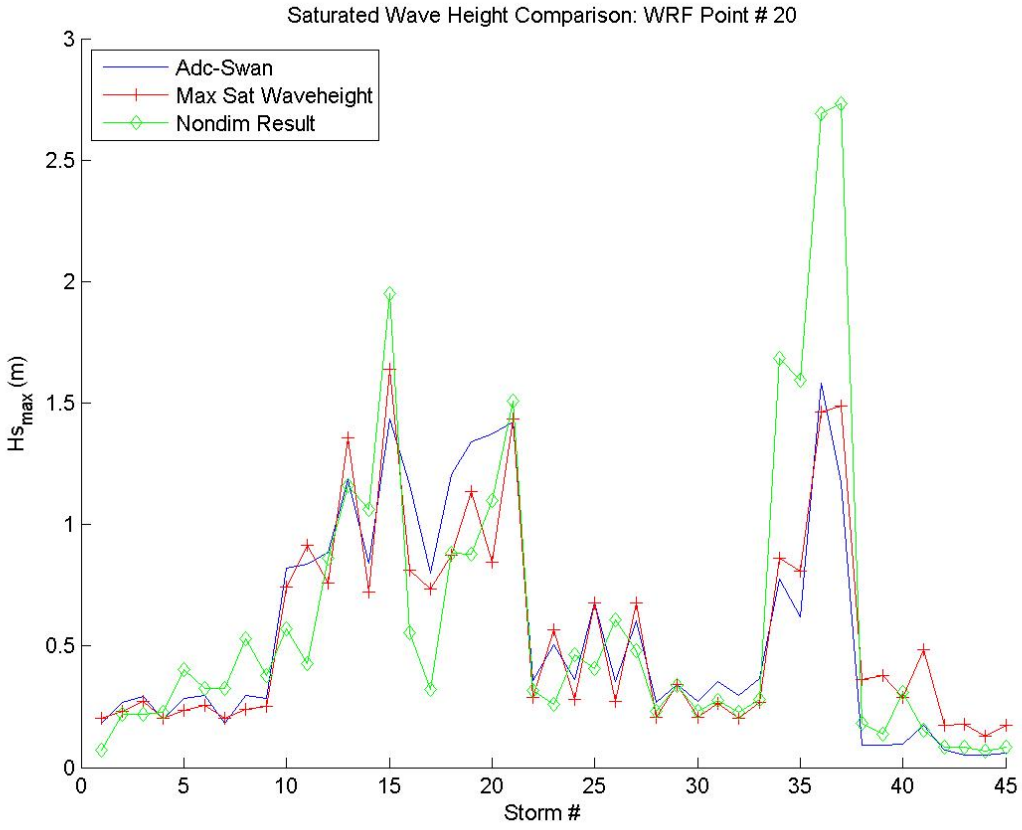

Figure 4.6 Comparison of wave heights predicted by: Model (blue), fully developed equations (red), and non-dimensional equations green.

Back prediction using the combined WRF methodology at bay locations was performed; RMSE, NRMSE's, and percent error (Equation. 4.11) were calculated, as well as bias for all locations. Bias is a typical statistic used in model validation (Ris et al. 1999, Rogers et al. 2006) and was calculated as seen in Equation 4.12.

$$Percent\ Error = \frac{1}{N}\sum_{i=1}^{N}\frac{(O_i - S_i)}{S_i} \tag{4.11}$$

$$Bias = \frac{1}{N}\sum_{i=1}^{N}(O_i - S_i) \tag{4.12}$$

where N is the total number of input data, O_i is the predicted H_s^{max} value and S_i is the modeled H_s^{max} value. Table 4.4 shows basic statistics for all bay and open coast locations, for all three test sites.

Table 4.4 Basic statistics for all sites, averaged across all bay stations.

Location	Bias (m)	NRMSE (%)	Percent Error (%)	RMSE (m)
Corpus Christi, TX	-0.09	17.1	14.0	0.31
Gulfport, MS	-0.07	12.4	23.4	0.21
Panama City, FL	-0.7	19.5	39.2	0.18

These results demonstrate the overall success of the WRF methodology application to the selected Gulf Coast sites. The maximum bias seen at any station was -0.25 m at Corpus Christi. As seen in Tab. 4.4 there is small bias introduced at any site. The NRMSE errors are small as well. The smaller NRMSE errors seen at Gulfport are likely a result of the larger range of wave heights seen at most Biloxi Bay stations. These back-bay stations (station #120-145) see very little wave height except under the most intense storms, resulting in a large range of H_s^{max}. Percent error calculations at all sites only considered storms causing wave heights greater than 0.5 m. Given the project goal of quantifying larger values for extreme value statistics and eventual damage calculations, maximum wave heights less than 0.5 m are less significant in this analysis. In addition, less intense storms cause extremely low wave heights at back bay stations at

all locations. In these cases, minute differences between the predicted wave height and the model wave height can cause very large percent error results, skewing the data set.

In addition to examining the basic mean statistics during analysis of bay stations, it was important to examine the spatial distribution of errors. This determined areas in which the WRF methodology performed well, as well as areas which need improvement. In order to do this, both the dimensional RMSE and non-dimensional percent error will be examined. Figures 4.7-4.9 show the spatial distribution of RMSE (m) and percent error for all three locations.

Noticeable differences are seen between error statistics in the two bay stations near the mouth of Biloxi Bay show lower percent error than those near the mouth of Bay of St. Louis. Back bay stations show larger percent error in both cases, ranging from 22-46% in the most sheltered areas. There are two likely reasons for this increased percent error at these back bay locations. First, the sheltered nature of these stations potentially reduces the correlation between storm characteristics and wave height. This can result in reduced accuracy via the non-dimensional equations, which are developed based on these dependencies. Second, modeled maximum wave heights at these are all below 2 m, so the small wave heights at these stations increase the percent error even though RMSE is low. Despite the increased percent error statistics at back-bay locations, the WRF method shows reasonable skill at all stations, keeping RMSE's at or below 0.4 meters in all locations.

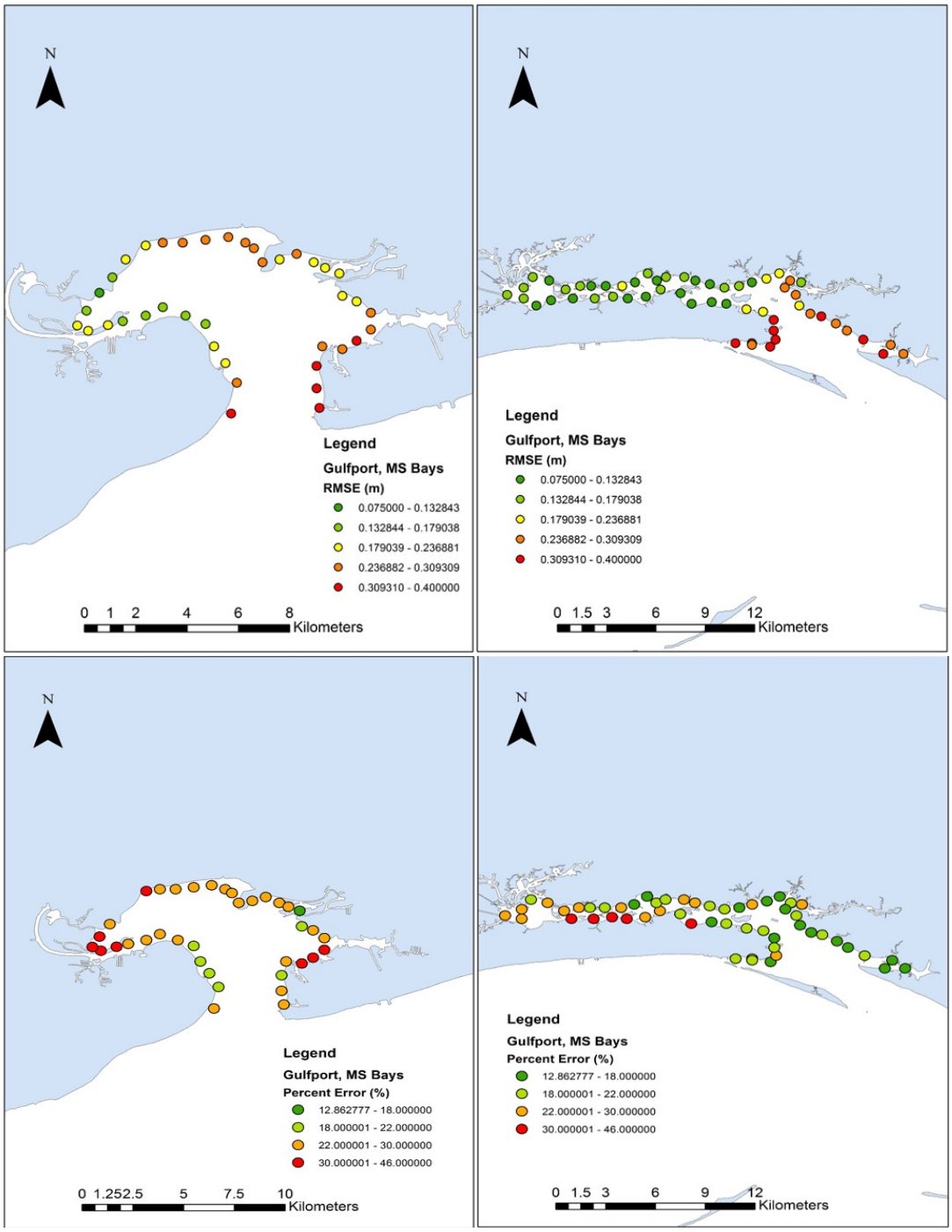

Figure 4.7 Clockwise from upper left: Bay of St. Louis RMSE (m), Biloxi Bay RMSE (m), Biloxi Bay Percent error, Bay of St. Louis Percent error.

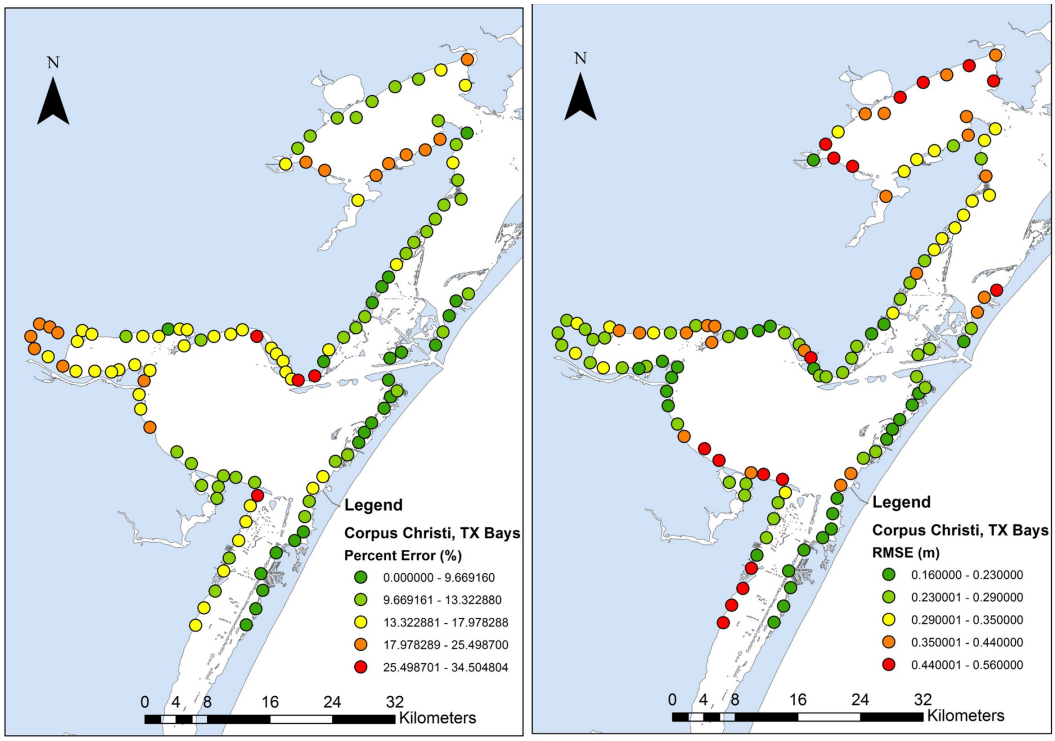

Figure 4.8 Left to right: Percent error at Corpus Christi, TX bay stations, RMSE error at bay station

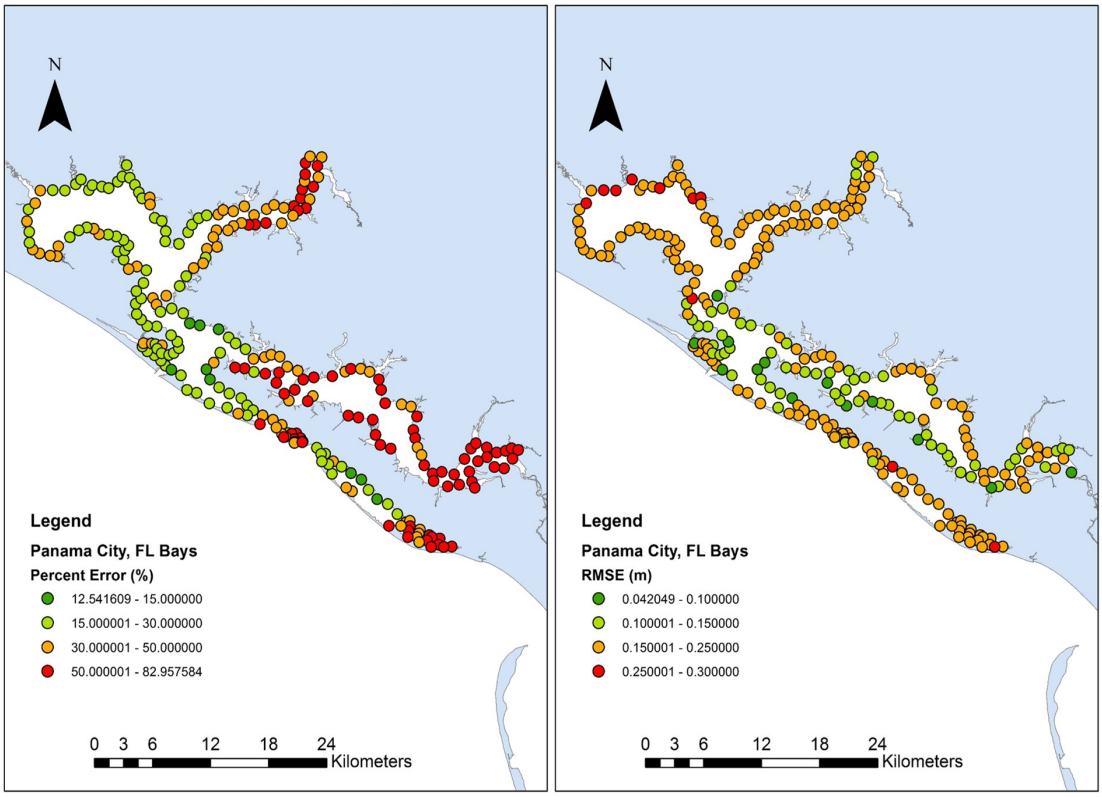

Figure 4.9 Left to right: Percent error at Panama City, FL bay locations, RMSE (m) at bay locations.

Error distribution throughout Corpus Christi Bay is similar to that of Biloxi and Bay of St. Louis at the Gulfport, MS site. Larger percent errors are seen at sheltered, isolated locations. Stations with percent error above 25.4% (red) are all located 1-3m above MSL. These landward stations have a much steeper profile. Steeper profiles often lead to surging breaker waves, which have very little dissipation and high reflection. This steep bathymetry may not reproduce the spilling breaker assumption inherent in the SWAN breaking model. This explains the increased percent error at these locations. Overall the WRF methodology shows skill, with RMSE below 0.35 meters at the majority of locations.

Analysis of errors at Panama City, FL yielded different results in many bay locations. The high percent errors at many stations is likely due to the consistently low wave heights experienced at these locations. Stations located in East Bay show much larger percent error than those in West Bay. Most of these East Bay stations never experience modeled wave heights above 1m. The consistently small waves at these stations shows the limited correlation between storm parameters and wave height. Given the overall project goal of parameterizing wave heights for extreme event analysis, the reduced skill at these stations is of lesser concern. Analysis results at these stations are shown for completeness. Stations in West Bay perform well, with most percent errors below 30% and RMSE values consistently below 0.25 m.

4.1.5 Open Coast WRF Methodology and Application

Open coast stations are subject to local wind waves, as well as swell that has been generated far offshore by the high velocity hurricane winds. These swell waves are formed over an "extended fetch" as detailed by Young (1988) and Alves et al. (2004). Due to the extended timeframe that many of these waves spend absorbing energy from hurricane winds, they are often much larger than bay waves. In order to determine how to best quantify open coast waves, an analysis procedure similar to that applied to the bay stations was performed. H_s^{max} RMSEs were compared for:

1. H_s^{max} predicted solely based on the non-dimensional equations.
2. H_s^{max} predicted solely based on the fully developed equations.

3. H_s^{max} predicted using the combined methodology described in Section 4.1.4.

Table 4.5 shows the mean RMSE for the three methods shown above.

Table 4.5 RMSE (m) for methods (1-3) described above, averaged over all open coast stations at each location.

Location	(Method 1)	(Method 2)	(Method 3)
Corpus Christi, TX	0.39	0.18	0.33
Gulfport, MS	0.53	0.23	0.34
Panama City, FL	0.33	0.18	0.28

The open coast results shown in Table 4.5 show substantially different results than the bays. Again, the non-dimensional formulation does not fare well on its own; however the combined method, which incorporates the non-dimensional forms as well as the fully developed equations, (method 3), fares much worse than solely using the fully developed equations (method 2). This is most likely due to the fact that under the intense hurricane winds and long fetches seen by open coast stations, there is much higher likelihood of a fully developed condition than the relatively sheltered bay stations. Therefore, the open coast stations solely utilize the fully developed equations, Equation. 4.6-4.8, during back predictions.

Back prediction using the fully developed portion of the WRF methodology at open coast locations was performed; RMSE, NRMSE's, and percent error (Equation. 4.11) were calculated, as well as bias for all locations. Table 4.6 summarizes the mean results across all open coast stations.

Table 4.6 Basic statistics for all sites, averaged across all open coast stations.

Location	Bias (m)	NRMSE (%)	Percent Error (%)	RMSE (m)
Corpus Christi, TX	-0.02	10.2	5.1	0.13
Gulfport, MS	-0.03	7.4	15.4	0.23
Panama City, FL	-0.1	10.63	9.73	0.18

Open coast predictions show almost no bias, with a maximum mean value of -0.03 m at Gulfport, MS. In addition, NRMSE are modest, with a lowest mean value of 7.4% in Gulfport, MS. Mean percent error is much lower than bay stations, with the lowest value being 5.1% in Corpus Christi, TX. Note that waves less than 0.5 m were again excluded from mean percent error calculations. RMSEs are well below that project goal of 0.3 m.

Open coast stations overall show better skill and lower errors than those seen at bay stations. Open coast stations are subject to waves directly forced by hurricane winds and unimpeded by inlets, barrier islands, or many of the other natural barriers that define bays. This results in higher correlation with storm parameters, and the lower errors detailed in Table 4.6. Similar to Section 4.1.4, spatial distribution of RMSE and percent error were analyzed at all open coast stations. Results are shown in Figures 4.10-4.12.

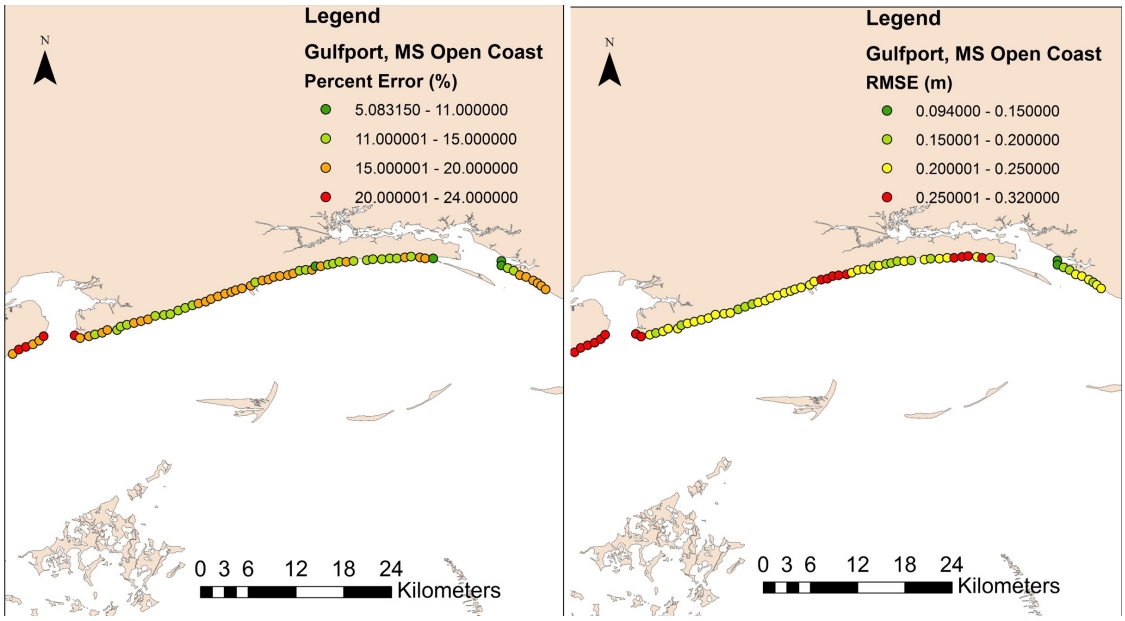

Figure 4.10 Spatial distribution of percent error (left) and RMSE in meters (right) at Panama City, FL open coast stations.

Spatial distribution of errors along the open coast shows one noticeable geographical trend. First, percent error (of modeled waves above 0.5 m) was greatest to the west of the Bay of St. Louis inlet. Percent errors in this region ranged from 15-24%, while RMSEs ranged from 0.25-.32 m, the highest seen at Gulfport open coast stations. Higher errors in this region could be due to the difficulty modeling the effect of the Mississippi River Delta on H_s^{max}. Although river discharge is included in the ADCIRC-SWAN model runs to which the WRF formulation is tuned, no explicit correction is made in the WRF method for delta's which could explain the increased error near the mouth of Bay of St. Louis. RMSE's are consistently below the project goal of 0.30 m, with a mean value of 0.23 m. Higher RMSE's compared to other sites can be attributed to the larger overall H_s^{max} values experienced at each station. The broad continental

shelf seaward of Gulfport, MS contributed to elevated surge levels, which lead to increased near-shore water depths allowing larger waves to propagate farther inland.

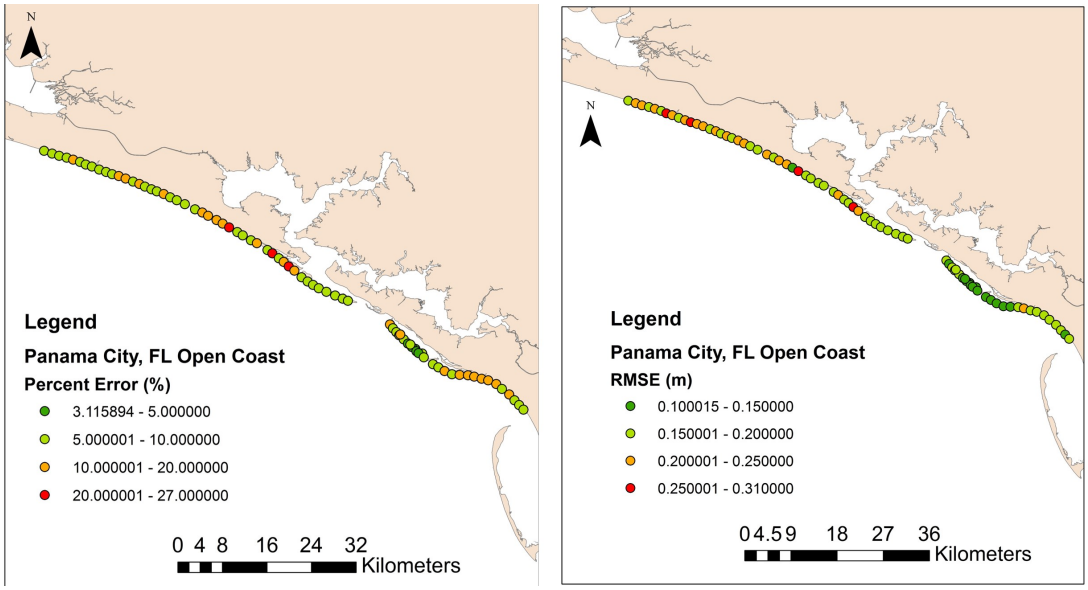

Figure 4.11 Spatial distribution of percent error (left) and RMSE in meters (right) at Panama City, FL open coast stations.

Panama City, FL open coast stations are well predicted overall. Most percent errors (of waves greater than 0.5 m) are below 20%, with more than half below of the stations below 10%. RMSEs are consistently below 0.30 m, with only 1 station greater (0.309 m). Spatial distribution of error shows no noticeable geographic trends.

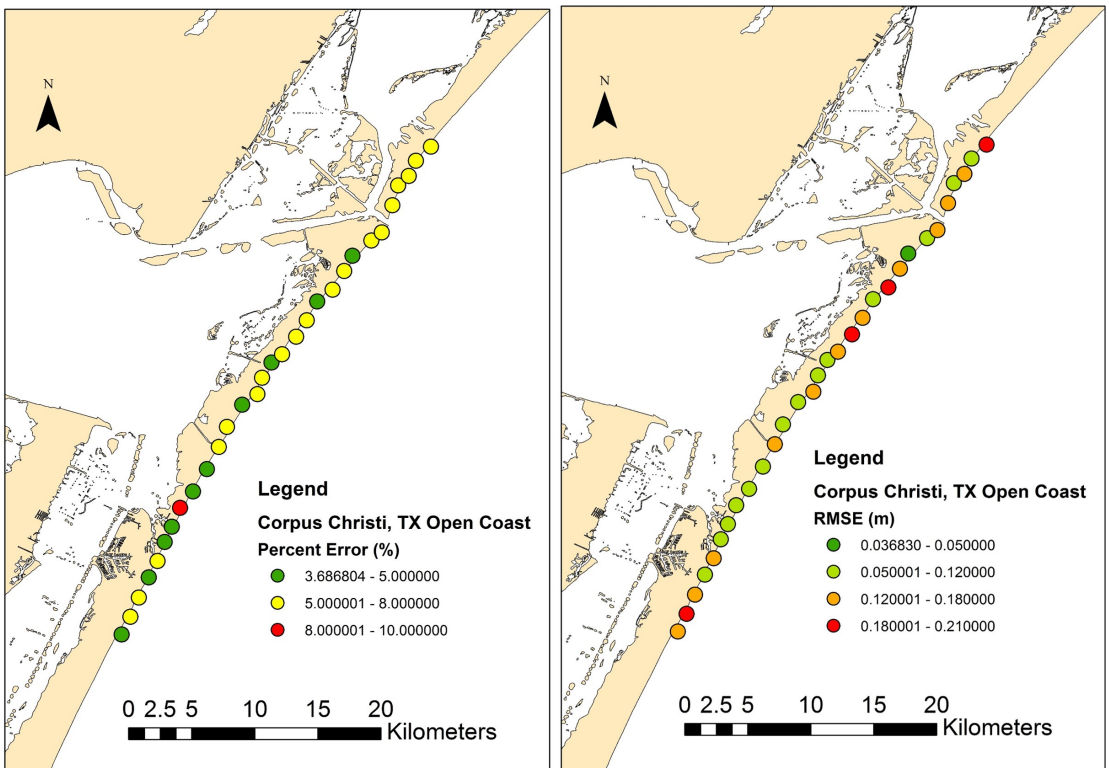

Figure 4.12 Spatial distribution of percent error (left) and RMSE in meters (right) at Panama City, FL open coast stations.

Corpus Christi, TX shows the lowest percent error of any location, with all stations below 10%. RMSEs are consistently below 0.20 m. Many Corpus Christi, TX stations are located on dry land, so weaker storms with lower surgelevels can lead to zero wave heights at these stations. When using the WRF method, when a zero surge occurs, wave heights are also zero. The exact prediction of the 0 m wave heights caused be these weaker storms causes lower the RMSEs observed at many stations.

4.2 Taylor (2012) Comparison and Hurricane Ike Data Validation

Previous WRF methods developed by Taylor (2012), discussed in Section 2.4 were applied to each station of interest. Wind speeds used in the Taylor model were calculated using the Holland (1980) model (Equation. 4.9-4.10). To quantify the performance of the Taylor model, RMSEs were calculated at each station and compared to those generated by the WRF method developed in this study. Table 4.7 shows a summary of average RMSE improvements over the Taylor (2012) methodology for both all locations.

Table 4.7 Summary of RMSE m averaged over all stations from the Taylor (2012) method and the WRF method discussed in this study. Improvement (m) from Taylor (2012) shown in last column

Location	Taylor (2012) RMSE	WRF RMSE	Improvement over Taylor (2012)
Corpus Christi, TX	0.50	0.20	0.30
Gulfport, MS	0.54	0.22	0.32
Panama City, FL	0.32	0.19	0.13

Average RMSE improvements range from 0.13-0.30 m. Comparisons of RMSE at the Corpus Christi, TX stations showed an overall average improvement of 0.30 m, with a 0.38 m average improvement at open coast locations and a 0.19 m improvement for bay stations. Gulfport, MS showed an overall average RMSE improvement of 0.32 m, with a 0.29 m average improvement at open coast stations and 0.34 m at bay stations. Panama City, FL showed an overall average RMSE improvement of 0.13 m, with a

0.143 m average improvements at both open coast and bay stations. Improvement in back prediction capability over the Taylor (2012) was apparent at all stations.

In addition to the improvements in accuracy over previous methods, the WRF method proposed in this study also has a greater dependence on physical hurricane parameters, which serves to tie the formulation closer to the physics of landfalling hurricanes. The elimination of the equivalent fetch term utilized in Taylor (2012) in the WRF method results in lower errors at inland bay locations, where fetch lengths (and the corresponding wave heights) have less correlation with a hurricane equivalent fetch. These stations are often subject to cross-bay winds (and thus short fetches) that generate waves rather than the extended open ocean distance that the equivalent fetch attempts to quantify. Open coast stations consider a fully developed condition, which directly accounts for near-shore dissipation processes (Verhagen and Young 1996a,b,c) unlike the Taylor (2012) method. In addition to the elimination of the equivalent fetch term, the WRF method directly considers minimum distance to storm track and station position relative to hurricane landfall location. With the highly variable winds within a hurricane, the distance from station to storm center has a substantial effect on H_s^{max}. In addition, the anticyclonic nature of hurricane winds and non-symmetric wave field distribution illustrate the importance of landfall position in wave height prediction. By considering D_{min} and landfall location, the WRF method better resolves H_s^{max} at all locations.

In order to properly evaluate any model, verification with field data should be performed where applicable. Kennedy et al. (2011) present one of the largest sets of

hurricane forced near-shore wave heights. In the Kennedy et al. (2011) study, eight rapidly deployable wave gauges were installed at various Gulf Coast locations. These wave gauges served to record free surface elevations, from which H_s^{max} values were calculated.

Mean depths of the stations ranged from 8.7-15.8 m over a 360-km section of coastline (Kennedy et al. 2011). Hurricane Ike was an especially large storm with a significant forerunner surge, which arrived well ahead of landfall (Kennedy et al. 2011); we note that the effects of this forerunner on near shore maximum wave heights are not included in the WRF formulation.

The WRF open coast method was used to calculate H_s^{max} at the location of all eight wave gauges. Maximum surge at each location was recorded via the wave gauges, and used to determine the maximum total water depth for input into the WRF formulation. Since data was only available at these locations for one storm, coefficients in Equation. 4.6 were not optimized and the standard coefficients found in Breugem and Holthuijsen (2007) were instead used. Another limitation of the Kennedy et al. (2011) data for this study was the large water depths. Depths used to formulate the WRF method were ~1-3 m, much less than the Kennedy et al. (2011) gauge location depths. Despite these limitations in the data set, back prediction yields favorable results. Figure 4.13 shows Hurricane Ike maximum recorded significant wave height back prediction.

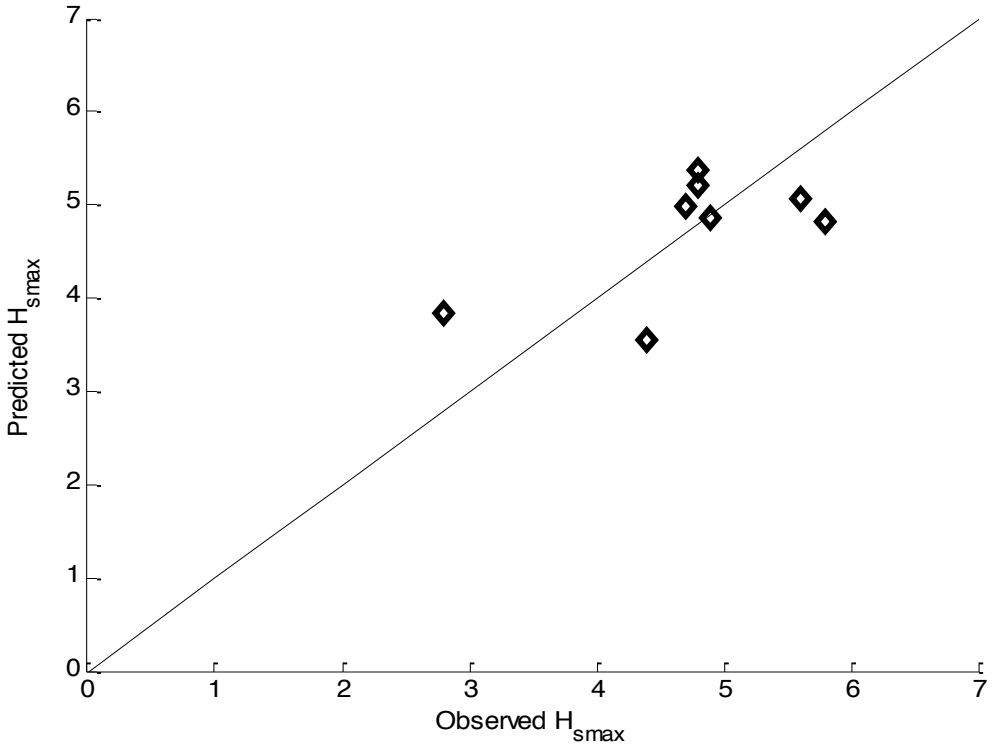

Figure 4.13 Back prediction results from the WRF method (Y-axis) vs recorded Kennedy et al. (2011) maximum significant wave heights (m). RMSE =0.67 (m).

Back prediction yielded a RMSE of 0.67 m. Although the RMSE in this validation is larger than those seen in earlier section, the method still displays skill. There are several likely reasons for the increased error. First, the WRF method was developed for near-shore conditions, utilizing the fully developed sea state equations developed previously (Verhagen and Young 1996, Breugem and Holthuijsen 2007). These equations were based on curve fitting equations developed based upon data taken in 2m of water. The WRF stations are in roughly 1-3 m of water. The large water depths of the Kennedy et al. (2011) gauges are not ideal for the WRF method, explaining

some of the increased error. Second, the WRF method relies on simulation of dozens of storms in order to properly optimize Equation. 4.6. Only one storm is available for this data set, so standard coefficients had to be used. Finally, the unique nature of the Hurricane Ike forerunner surge resulted in maximum water depths that occurred before hurricane landfall. The WRF method assumes relatively concurrent occurrences of maximum surge and wave height, as detailed in Section 4.1.2. The historical forerunner surge could also be a source of some of the error seen in Figure 4.14. Despite these limitations, the WRF method displays reasonable skill when compared to the Hurricane Ike field data of Kennedy et al. (2011).

4.3 Conclusions of WRF Parameterization Study

Presented in this section are development, application, and validation of the WRF maximum wave height response model. Development of the WRF method considered which storm parameters are necessary for accurate parameterization of H_s^{max}. Parameters included in the non-dimensional formulation include D_{min}, ΔC_p, R, surge depth, and bathymetric depth. Landfall location is included by grouping curve fits into left, right, and middle categories, defined relative to the location of landfall. It was apparent that sole use of the non-dimensional equations did not yield sufficiently skillful back predictions at larger (greater than 2 m) waveheights, so a fully developed sea state cap based on the work of Verhagen and Young (1996) and Breugem and Holthuijsen (2007) was included. This is used in conjunction with the non-dimensional equations at

bay stations, and alone at open coast locations. Finally the WRF method was compared to Taylor (2012) methods and validated using Kennedy et al. (2011) Hurricane Ike data.

The WRF proves a computationally efficient, skillful method for parameterizing hurricane induced maximum significant wave heights. RMSEs are consistently below 0.30 m, and percent errors mostly below 20-30%. Problems in the WRF method arise when resolving wave heights at open coast locations near river deltas, as seen in the westernmost open coast stations in Gulfport, MS. The WRF method does not resolve wave heights at bay stations where wave heights are consistently low, resulting in much higher percent errors at these locations. However given the project goal of analyzing extreme values, error in these locations is of lesser concern. The equations and methodologies described in this section can be used to analyze extreme value statistics as detailed in the following section.

5. WRF APPLICATION TO EXTREME VALUE STATISTICS

5.1 JPM-OS: Methodology and Surge Application

The Joint Probability Method with Optimal Sampling, JPM-OS, has been applied in estimating extreme value probabilities of hurricane induced surge. Extreme value statistics generated by traditional Joint Probability Methods, JPM, first developed by Ho and Myers (1975) strongly depend on the individual probability distribution of input parameters. The input parameters traditionally used in hurricane extreme value analysis include, central pressure, storm size, forward speed, and approach angle (Myers 1975; Ho and Myers 1975). This introduces substantial computational burden. For example, if five values of C_p, R, v_f, and θ along five tracks are to be analyzed, 3125 storms need to be simulated. Given an average ADCIRC-SWAN runtime of roughly 12 computational hours, this would take around 130 days of runtime to complete. In order to develop a more computationally efficient way to evaluate extreme value statistics via the JPM, JPM-OS was developed (Resio et al. 2009). Optimal sampling involves simulating a smaller set of representative storms which fill the larger parameter space. Once a representative suite of storms is chosen for a given test site, SRFs, introduced by Irish et al. (2009) are developed. SRF's serve as a computationally efficient method of parameterizing hurricane peak surge, and quickly simulating the thousands of storms necessary for extreme value analysis via the JPM-OS. In this study, parameterized WRFs developed in Section 5 are applied in a similar manner to analyze extreme value

wave statistics in the near shore environment. Application of the JPM-OS technique involves first determining the maximum condition at a given station. Previous applications by Resio et al. 2009 used Equations 5.1 and 5.2 to form a flood response model:

$$z_{max}(x) = \phi\left(x, \Delta C_p, R_p, v_f, \theta, x_o, MSL\right) + \varepsilon_z \quad (5.1)$$

$$\varepsilon_z^2 = \varepsilon_{tide}^2 + \varepsilon_{surge\ simulation}^2 + \varepsilon_{waves}^2 + \varepsilon_{winds}^2 + \cdots. \quad (5.2)$$

Where:

ϕ is a continuous flood response function

x is location of interest

x_o is landfall location

R_p is hurricane pressure radius near landfall (Thompson and Cardone, 1996)

Θ is the hurricane approach angle with respect to the shoreline

v_f is the hurricane forward speed near landfall

MSL is the mean sea level

ε_z is the epistemic uncertainty in the flood response (Resio et al. 2009)

Resio et al. (2009) limit the number of dimensions to those within the PBL model. They argue that the hurricane wind field generated by the PBL model have provided accurate estimates of ocean responses to hurricanes in the Gulf of Mexico. Since the WRF methodology relies upon the wind field predicted from the Holland (1980) formulation, a similar assumption can be made for analysis of waves. Equation 5.2 represents any uncertainty due to unspecified tides and error in model inputs, wind inputs, etc.

Early JPM applications relied upon discrete probability densities. Irish et al. (2011) use continuous probability density functions to represent the distributions of each parameter of interest. They assume an extreme value Gumbel distribution to represent central pressure (Equation. 5.3) and normal distribution to represent radius, forward speed, approach angle, and landfall location (Equation. 5.4-5.8), expressed as follows:

$$\lambda_1 = p(c_p|x_o) = \frac{1}{a_1(x_o)} \exp\left[-\frac{\Delta p - a_o(x_o)}{a_1(x_o)}\right] * \exp\left\{-exp\left[-\frac{\Delta p - a_o(x_o)}{a_1(x_o)}\right]\right\} \ (Gumbel\ Distribution) \tag{5.3}$$

$$\lambda_2 = p(R_p|c_p) \tag{5.4}$$

$$= \frac{1}{\sigma(\Delta p)\sqrt{2\pi}} \exp\left\{-\frac{\left(\overline{R_p}(\Delta p) - R_p\right)^2}{2\sigma^2(\Delta p)}\right\} \ (Normal\ Distribution)$$

$$\lambda_3 = p(v_f|\theta) = \frac{1}{\sigma\sqrt{2\pi}} \exp\left\{-\frac{\left(\overline{v_f}(\theta) - v_f\right)^2}{2\sigma^2}\right\} \ (Normal\ distribution) \tag{5.5}$$

$$\lambda_4 = p(\theta|x_o) \tag{5.6}$$

$$= \frac{1}{\sigma(x_\square)\sqrt{2\pi}} \exp\left\{-\frac{(\bar{\theta}(x_o) - \theta)^2}{2\sigma^2(x_o)}\right\} \ (Normal\ Distribution)$$

$$\lambda_5 = f(\lambda, x_o) \tag{5.7}$$

where:

λ_i = probability density function for each parameter

a_0, a_1 = Gumbel coefficients

σ = standard deviation of normal distribution

$f(\lambda,x_o)$ = rate of landfall occurrence per unit length of coast.

In Equation 5.7, $f(\lambda,x_o)$ represents the probability of hurricane landfall at a given location. Normal distribution mean values are represented by overbars.

The continuous probability density function, p, for the combined set of parameters is then:

$$p(c_p, R_p, v_f, \theta, x_o) = \lambda_1\lambda_2\lambda_3\lambda_4\lambda_5 \quad (5.8)$$

Irish et al (2011) reduced this combined JPM probability density function to rely solely on the influences of central pressure, storm size, and landfall location. This reduction of the parameter space was based upon Irish et al. (2008), which showed that the influence of forward speed and track angle have minimal effects on peak surge when compared to other parameters. Here, the track angle must be included, as it will be used to form a straight line approximation of the storm track in order to calculate D_{min}, the minimum distance between point of interest and storm track (as defined in Section 4.1.2).

Once the probability density function is determined, the resulting surge from each synthetic storm simulated is interpolated to a finer resolution, which represents the entire JPM space. See Table 5.1 for complete list of storm simulated and JPM parameter resolution. Table 5.1 represents the JPM resolutions chosen for Panama City, FL. Subsequent analysis at other locations will require site specific examination and tuning.

Table 5.1- Resolution chosen for each parameter used in JPM-OS calculations. Format is as follows: (minimum value:step:maximum value)

Resolution	C_p (mb)	R (km)	θ (degrees)	x_o
Storm	770:20:970	7.4:7.4:119	-80:5:10	400:5:665
JPM	770:5:970	7.4:1:119	-80:5:10	400:5:665

Interpolation of surge values from the storm set to the JPM resolution space was followed by computation of the surge probabilities, and subsequent return period calculations. A user specified surge interval is selected, and the probability density function is summed over each surge interval. The surge interval is selected based on range of surge at a given location. The result is a cumulative distribution function for the surge. Return Period charts can then be produced, and extreme value statistics analyzed at each station of interest. Figure. 5.1 shows example surge return period curves for Panama City, FL. These curves show increasing surge level with increasing return period. Higher surge levels are observed at open coast locations. Bay locations show similar trends, with lower overall surge observed. Application of the JPM methodology to extreme value wave statistics was performed similarly to surge. The following sections examine how to implement the JPM-OS methodology to extreme value statistics analysis for waves.

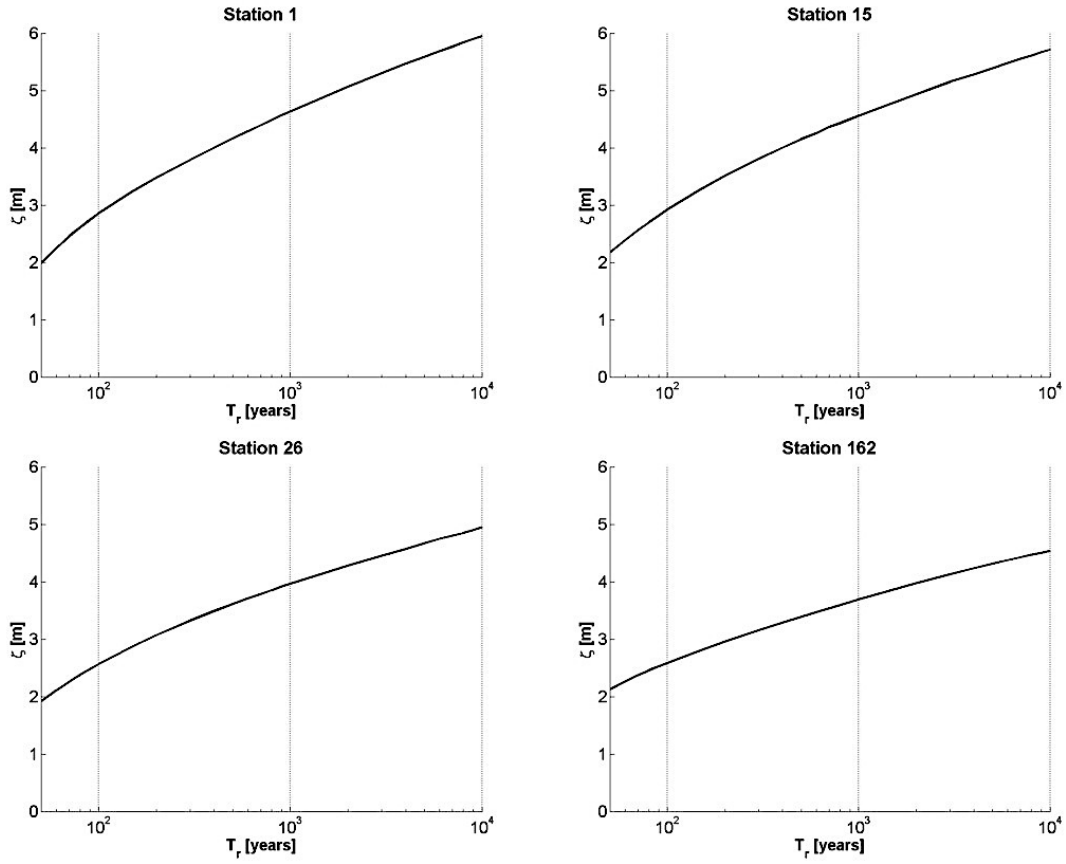

Figure 5.1 Surge return period curves for bay and open coast stations. Top row shows open coast stations 1 and 15, while bottom row shows bay stations 26 and 165.

5.2 JPM-OS Application to Panama City, FL Waves

In this study, the JPM-OS methodology described in Section 5.2 will be used to analyze extreme value wave statistics. Using the same methodology for wave statistics as for surge involves assuming that the physical dependencies for waves are the same as that of surge. While the physics of surge generation are different from those of waves, many of the same forcings apply, and the JPM-OS can be used as an initial proxy of extreme value statistics for hurricane driven waves. For example, key parameters in the surge JPM-OS include central pressure, storm size, forward speed, approach angle, and landfall position. These are spaced at different intervals, detailed in Table 5.2, to comprise the thousands of synthetic storms simulated with the SRF methodology. Central pressure, storm size, and landfall position are explicitly taken into account in the WRF methodology. Although approach angle is not directly included in the WRFs, it will be used during this analysis to form a straight-line track from which D_{min} can be approximated. After the WRF methodology was applied to each station as detailed in Section 5, it was used to simulate the thousands of synthetic storms necessary to begin analysis using the JPM-OS. The steps for maximum significant wave height extreme value analysis via JPM-OS is as follows:

1. Determine set of representative storms for optimum sample. These should span the parameter space for a selected location. Simulate these storms via ADCIRC-unSWAN, or another suitable model configuration.

2. Develop WRFs based upon Section 5 and SRFs based upon Irish et al. (2009), Song et al. (2012), and Resio et al. (2013).
3. Simulate the thousands of necessary storms for JPM-OS using the functions from step 2. Do this for surge and waves. (Note that wave JPM-OS analysis of each synthetic storm requires the corresponding surge value as input into the WRF formulation)
4. Apply JPM-OS using 4-term parameter space. (c_p, R_p, θ, x_o)
5. Analyze data and return period curves for extreme value statistics.

Results of the JPM-OS applied to Panama City, FL are shown for open coast and bay stations in Figure 5.2. This plot shows return period curves for 4 Panama City, FL stations.

Analysis of both wave and surge return period curves begins at the 50 year storm. This is due to the nature of the JPM-OS methodology. Fitting of probability distributions and subsequent calculations of the continuous probability density function emphasizes extreme value statistics (Resio et al. 2009). Therefore, shorter return period wave heights and surges, (less than 50 years), were not analyzed and are absent from Figure 5.1-5.2.

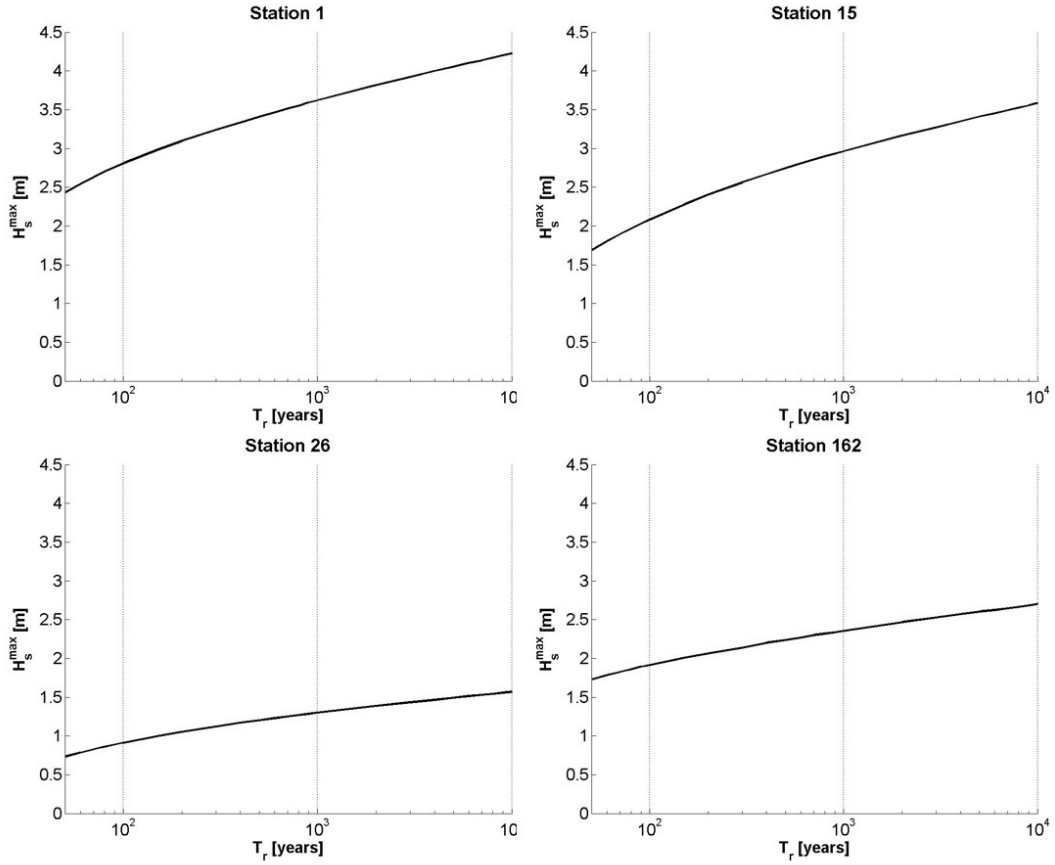

Figure 5.2 Wave return period curves for bay and open coast stations. Top row shows open coast stations 1 and 15, while bottom row shows bay stations 26 and 165. Note the significantly lower bay wave heights when compared to the surge levels seen in Fig. 5.1.

It should be noted that the JPM-OS assumes a correlation between storm parameters and the parameter investigated. When applied to wave statistics many of the Panama City, FL back-bay stations have small wave heights, no matter the storm conditions. These stations rarely experience waves over 1 m, as detailed in Section 4.1.4. This limited relationship between storm parameters and wave heights reduces the reliability of JPM-OS extreme value estimates at these stations. Future analysis and corrections to the JPM-OS methodology may be needed to accurately portray the extreme value statistics at these stations. Events with return periods of 50, 100, and 500 year events were analyzed for 179 open coast and bay stations. Maximum wave heights and surge levels are shown in Table.5.2.

Table 5.2 Maximum surge and wave levels seen for 50, 100, and 500 year return periods, split by bay (top) and open coast (bottom) locations.

Return Period [years]	Bay Maximum Surge [m]	Bay Maximum Wave [m]
50	2.9	1.1
100	3.7	1.3
500	5.0	1.5
Return Period [years]	Open Coast Maximum Surge [m]	Open Coast Maximum Wave [m]
50	2.4	2.3
100	3.1	3.3
500	4.1	4.3

Maximum wave events at bay stations shows a more gradual increase with increasing return period when compared to the maximum surge. This indicates less correlation between increasing storm intensity and wave height. Open coast stations

show similar increasing patterns, illustrating the increased relation between storm parameters and wave height at open coast stations. Although wave events exceed surge levels for the 100 and 500 year storms, wave height to total depth ratios do not exceed 0.65 in any locations. Monochromatic waves tend to break when this ratio reaches ~0.78 (Dean and Dalyrymple 2002); therefore these wave heights were deemed reasonable.

H_s^{max} levels for the 100 year event are shown in Figure 5.3 for all Panama City, FL stations. Fewer stations were used for JPM-OS analysis than WRF analysis. A total of 178 out of the 346 WRF stations were selected for JPM-OS analysis. This was done to minimize computational time while maintaining a dense spatial resolution.

H_s^{max} levels at western open coast stations are generally in the 2.1-3.4 meter range, with stations to the east mostly below 2 meters. Bay stations show great variety, with those directly behind barrier islands mostly 0.31-2.0 meters. Stations located in east bay show extremely low wave heights, with many below 0.15 m and all below 0.3 m. These back bay stations continually show low wave heights no matter the storm parameters. Extreme value analysis at these stations, therefore, has limited application under the current methodology. Wave heights remain constant with increasing return period at these stations. West bay stations show greater correlation to storm parameters, and wave heights gradually increase with T_r.

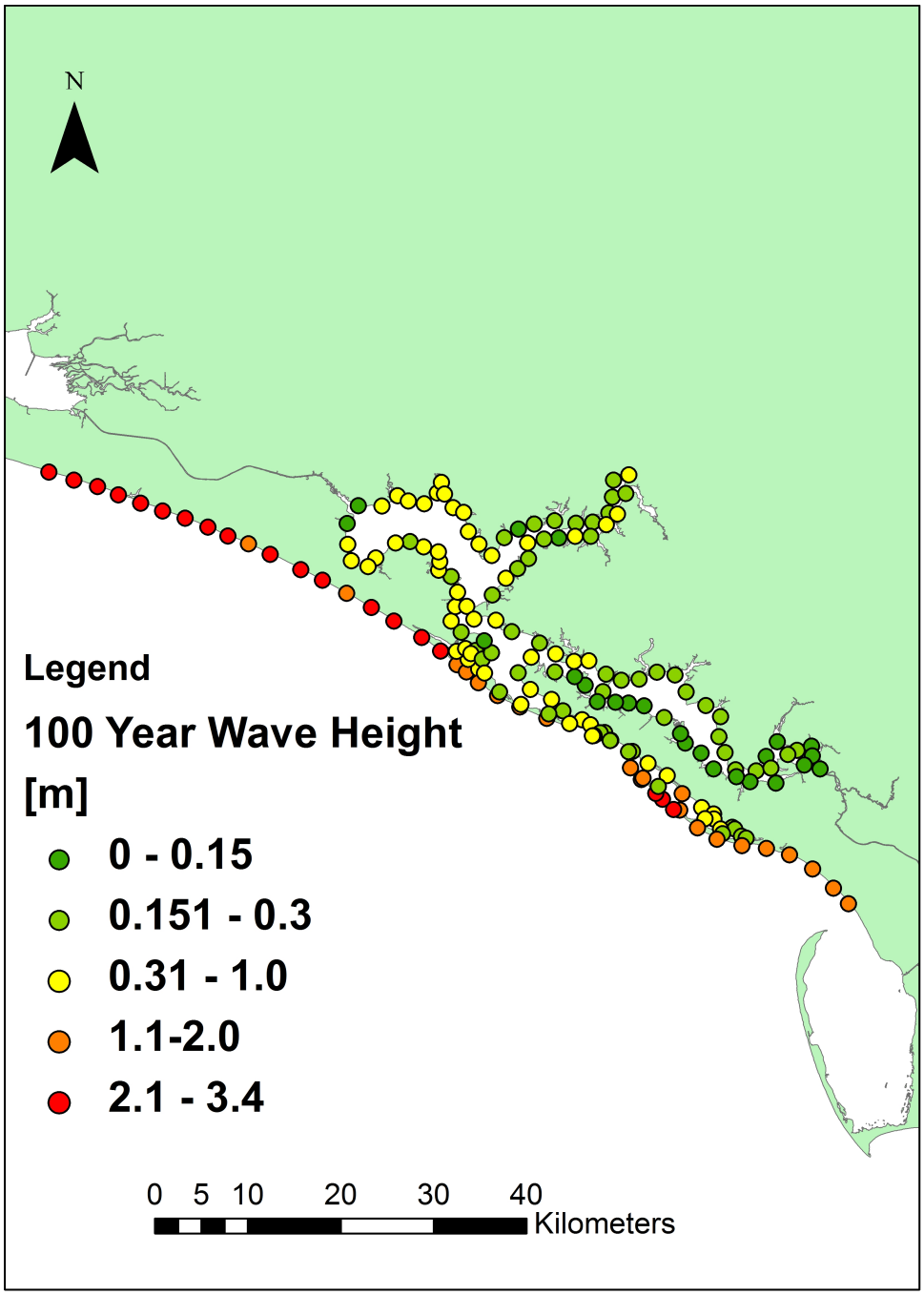

Figure 5.3 100 year maximum significant wave height for all Panama City, FL stations.

5.3 Projecting Wave Heights onto Land for ArcGIS Analysis

In order to perform damage vulnerability and risk calculations for coastal communities, it is necessary to have a spatially dense prediction of extreme events such as surge and wave heights over land. This would involve projection of the surge or wave event from the coastline onto areas not normally inundated. Once the surge or wave event is projected over land, further social and economic analysis can be performed. Currently, methods to project surge over land are limited to model results such as ADCIRC using a wetting and drying algorithm for near shore nodes (Leuttich and Westerlink 1999). When coupled with a wave model, ADCIRC-SWAN can project waves over land as well. Although accurate, this methods present problems for determining accurate extreme value statistics via the JPM method, mostly the excessive computational times required for model runs.

Once extreme value statistics are analyzed via the JPM-OS using WRFs developed in this study, projection of these wave events onto inundated areas is necessary. Surge and wave levels are only calculated at each station, requiring delineation of areas influenced by each station. The extreme value surge level must be distributed to adjacent landmass areas for damage analysis. Currently, no there are no published methods of delineating a region affected by each WRF point. The methodology for projected surge near shore coastal areas presented in this section is the direct work of PhD candidate Chih-Hung Hsu (personal consultant). His "SRF Zone" GIS methodology is as follows:

1. Use each SRF point to create Thiessen polygons. Limit these polygons to only the ocean part. This will delineate the shoreline affected by each near shore SRF station (Figure 5.4)

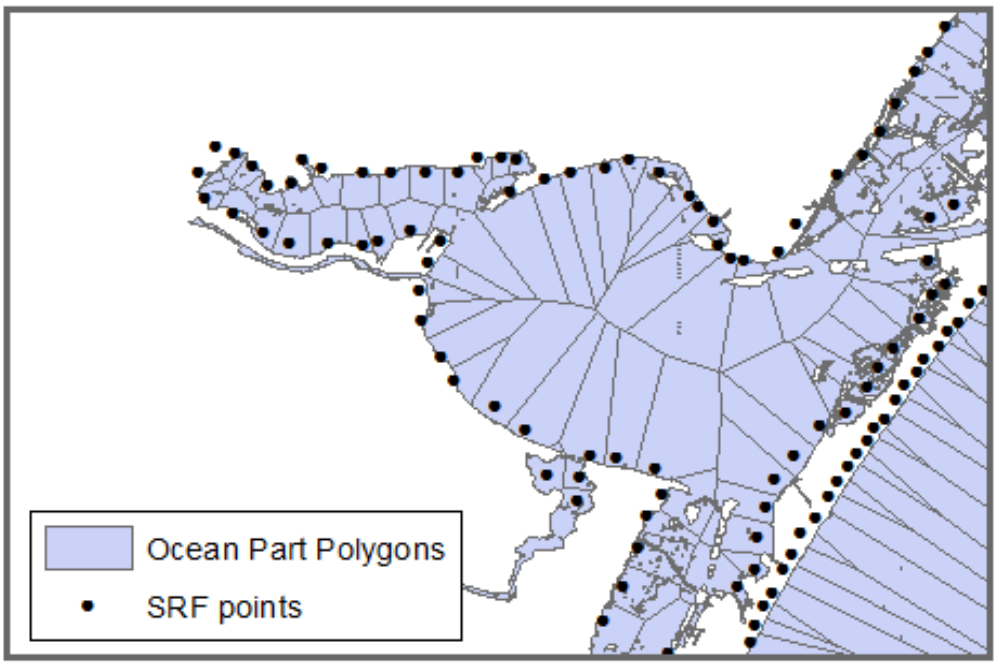

Figure 5.4 Thiessen polygons for shoreline watershed delineation. Application to Corpus Christi, TX. Figure and method by PhD student Chih-Hung Hsu (AaronHsu@tamu.edu).

2. Treat a specified point on each shoreline as a watershed outlet. A watershed is defined as the region which drains to a specified outlet.
3. Create pour points along Thiessen polygon shoreline using ArcGIS. This an ArcGIS function that will pick the point along each shoreline that will result in the greatest watershed area. This is to prevent unrealistically small watersheds created by poorly chosen outlet points.

4. Delineate watersheds based on each pour point. Since the outlet is the shoreline affected by the surge associated with the corresponding SRF point, the watershed will be landmass area affected by each SRF station.
5. Create Polygons for each watershed. These will be the SRF polygons, the landmass area affected by surge levels at each SRF station (Figure 5.5)

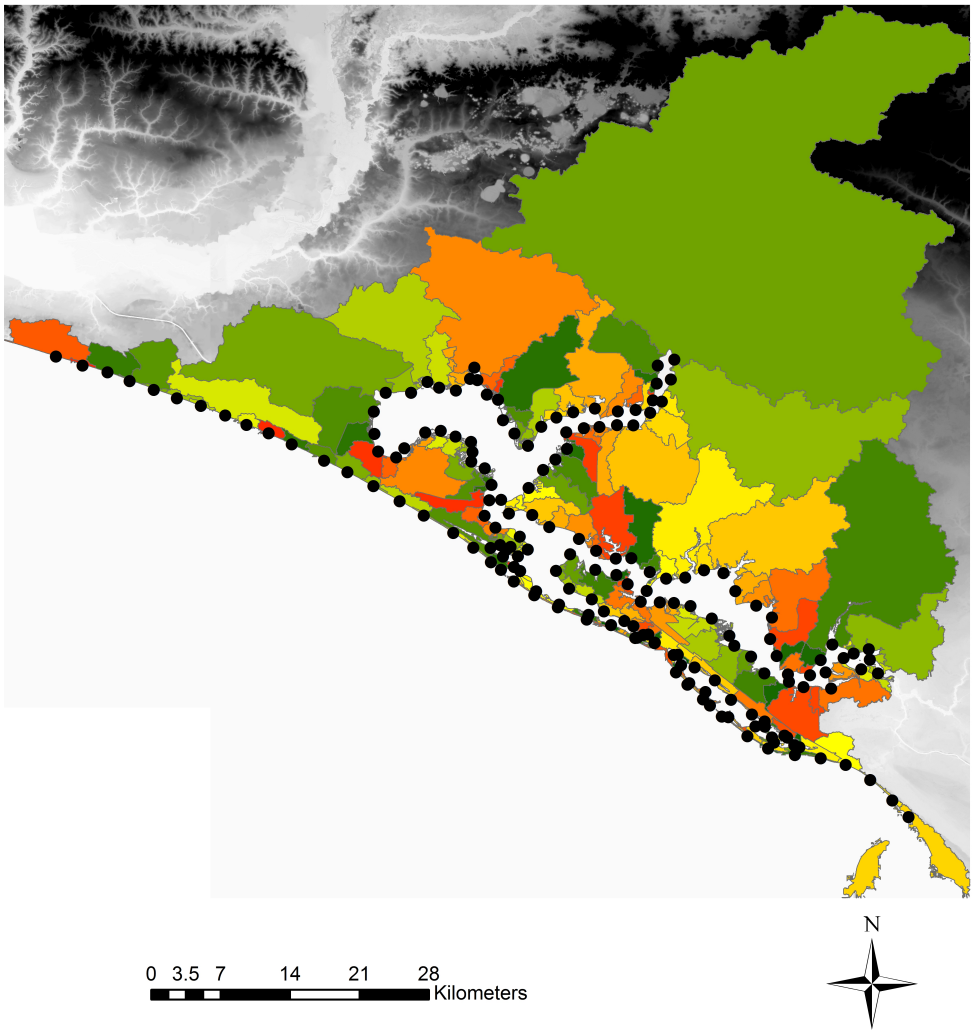

Figure 5.5 SRF zones for Panama City, FL. Each zone has a corresponding station where surge data is calculated and distributed through the zone using the Hsu methodology.

The Hsu SRF zone methodology was used to create SRF zones for Panama City, FL. 179 SRF zones were created, corresponding to each point from the JPM-OS analysis. Digital Elevation Maps, or DEM, files are overlain with the SRF zones, and extreme event surge levels from each SRF station are projected as a flat level line over each corresponding SRF zones. Flood depths at each raster cell, are calculated as the surge depth minus the DEM elevation.

The Hsu formulation is developed with surge calculations in mind. By treating each point as a watershed outlet, surge levels over land are easily approximated. Although the Hsu methodology was developed for surge levels, it will be used to approximate wave levels over the landmass. By using the same SRF zones to approximate the area affected by wave events at each station, the effects of processes that could change the area of landmass affected such as refraction and diffraction are ignored. Despite this limitation, using the same zones will simplify analysis and reduce computational time. In addition, inundation depths over land were used to calculate wave levels, so using the same method of projecting flood levels onto land is intuitive. Stations used to create the SRF zones are spaced at intervals (~2km) such that surge is slowly varying from station to station, and any discontinuities at the overland boundaries between zones is minimal. Waves are less slowly varying, as there are sharp drops in wave heights from open coast locations to bay stations sheltered by land. Although discontinuities may occur at the interface between open coast and bay based SRF zones, it is necessary to use the same methodology for waves, since wave heights predictions are tied to surge levels, as further discussed in the wave analysis projection method later

in this section. In addition, this is physically valid, except at exact boundary lines between zones, because on land areas influenced by bay surge are subject to shorter fetches and less wave forcing than those influenced by open coast surge and wave conditions

Wave analysis over flooded land was conducted as follows:

1. Use the Hsu methodology outlined earlier in this section to create SRF Zones.
2. Project selected surge extreme events over each SRF zone.
3. Calculate total water depth for 100 year surge (bathymetric depth + surge level)
4. Calculate ratio of 100 year wave height to total water depth at each station, for each selected extreme event.
5. Assume ratio calculate at each station to be constant within corresponding SRF zone. Use this to calculate the wave height at each flooded cell.
6. Produce spatial maps detailing extreme event wave heights over flooded, on land areas.

In order to assume that the 100 year surge can be used to calculate the 100 year wave height to total depth ratio (step 4), it was important to investigate the similarity of the JPM storms that produce similar return period surges and waves. Storms within the JPM parameter space (see Tab 5.1) were analyzed for storms that resulted in surges within 10% of the 100 year event level. The same process was done for waves. Then the two storm sets were compared to see which percentage of storms created values

within 10 % of the 100 year event level. Figure 5.6 summarizes the findings, as well as investigating the 20% level.

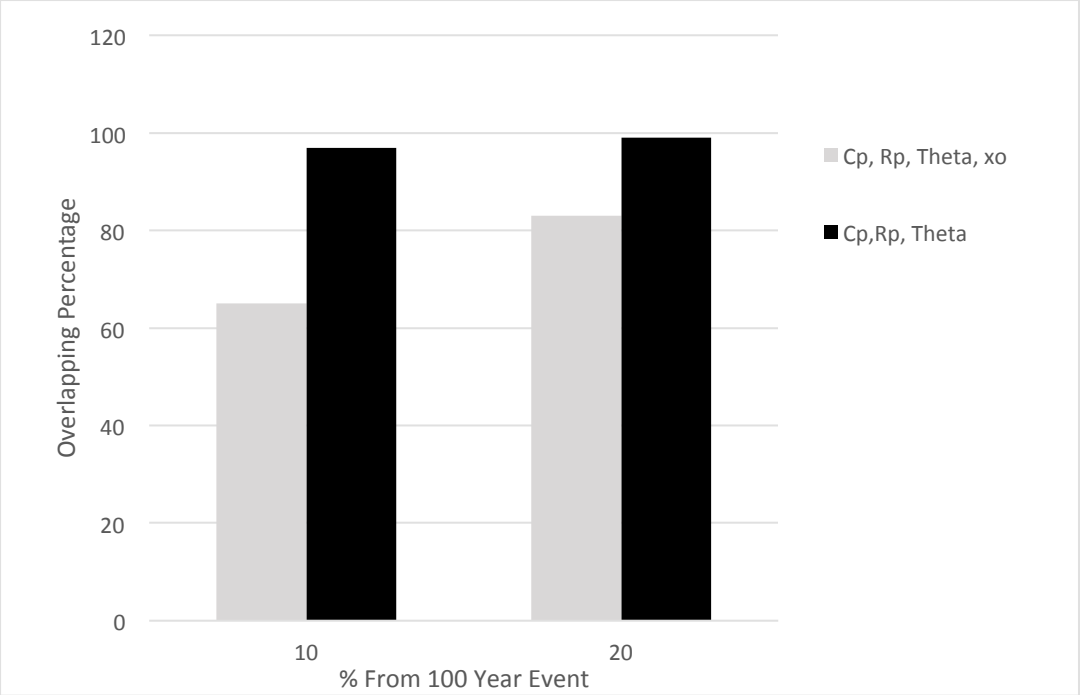

Figure 5.6 Percentage of overlapping storm events between 100 year surge and wave events, determined by analyzing JPM storm inputs. Analyzed for all storms within 10 % (left) and 20 % (right) of the 100 year level. Shown for all storm parameters (black) and excluding x_o parameter.

It can be seen that 65% of the storms scenarios causing surges and waves within 10% of the 100 year elevation. This means that 65% of the time, the 100 year event for both surge and waves is caused by an exactly similar storm. This increases to 97% of storms when the landfall position parameter x_o is removed. This is most likely due to the differing spatial distribution of surge and wave fields. When focusing solely on storm characteristics (C_p, R_p, θ) and excluding the spatial characteristics (x_o), events

contributing to the 100 year wave height and 100 year surge levels are very similar. Similarity between storm sets causing the 100 year event increases to 83% when considering all storms causing surge and wave levels 20% from the 100 year event. This increases to a similarity of 99% of storms when the landfall position parameter x_o is removed from consideration. These results show that most of the variability between events causing the 100 year surge and 100 year wave height is due to the x_o parameter. Tables 5.3 and 5.4 summarize the return period range for the 10% band for surges and wave, respectively.

Table 5.3 Return period equivalent for +/- 10% of 100 year surge level.

Percent Change	T_r [years]	Surge (m)
+10%	145	2.55
0	100	2.32
-10%	72	2.09

Table 5.4 Return period equivalent for +/- 10% of 100 year wave level.

Percent Change	T_r [years]	Wave (m)
+10%	157	2.62
0	100	2.38
-10%	68	2.14

Application of the method described earlier in this section is physically reliable due to the relatively large overlapping percentages seen in Figure 5.6, especially when considering only storm characteristics.

Limitations of this methodology are mostly due to the assumption of a constant ratio of wave height to water depth within each SRF zone. This assumes the effects of

changes in bottom roughness and bathymetry due to onshore obstructions has no affect on this ratio. However this simple calculation will yield a quick and accurate of approximation of onshore wave levels due to extreme storm events, a prediction previously only available from computationally expensive model runs. Additionally, this methodology allows for addition of a more sophisticated description of breaking and its relation to onshore depth. Figures 5.7-5.8 shows the 100 and 1000 year wave events for all flooded onshore cells. Figures 5.7-5.8 show continually low wave heights in the East Bay. This is due to the continually low wave heights seen in this area in the ADCIRC-SWAN model results. This suggests that wave heights in this area are at lower risk to hurricane wave damage. Open coast locations see less flooding due to the steep near shore profile, resulting in the limited inundated area in Figures 5.7-5.8. These results can be overlain with parcel data to perform combined surge and wave damage and risk analysis.

These maximum wave height maps can be generated for any return period of interest using the methodology outlined in this section. Although a simple approximation of hurricane forced onshore wave events, this methodology allows extremely fast and computationally efficient generation of spatially dense maximum wave height maps. For example, once appropriate input files are generated, all calculations in this section can be performed in under an hour of computational time on a standard home personal computer. Future advancement of this application should involve creating wave specific WRF zones so issues at the boundaries are resolved.

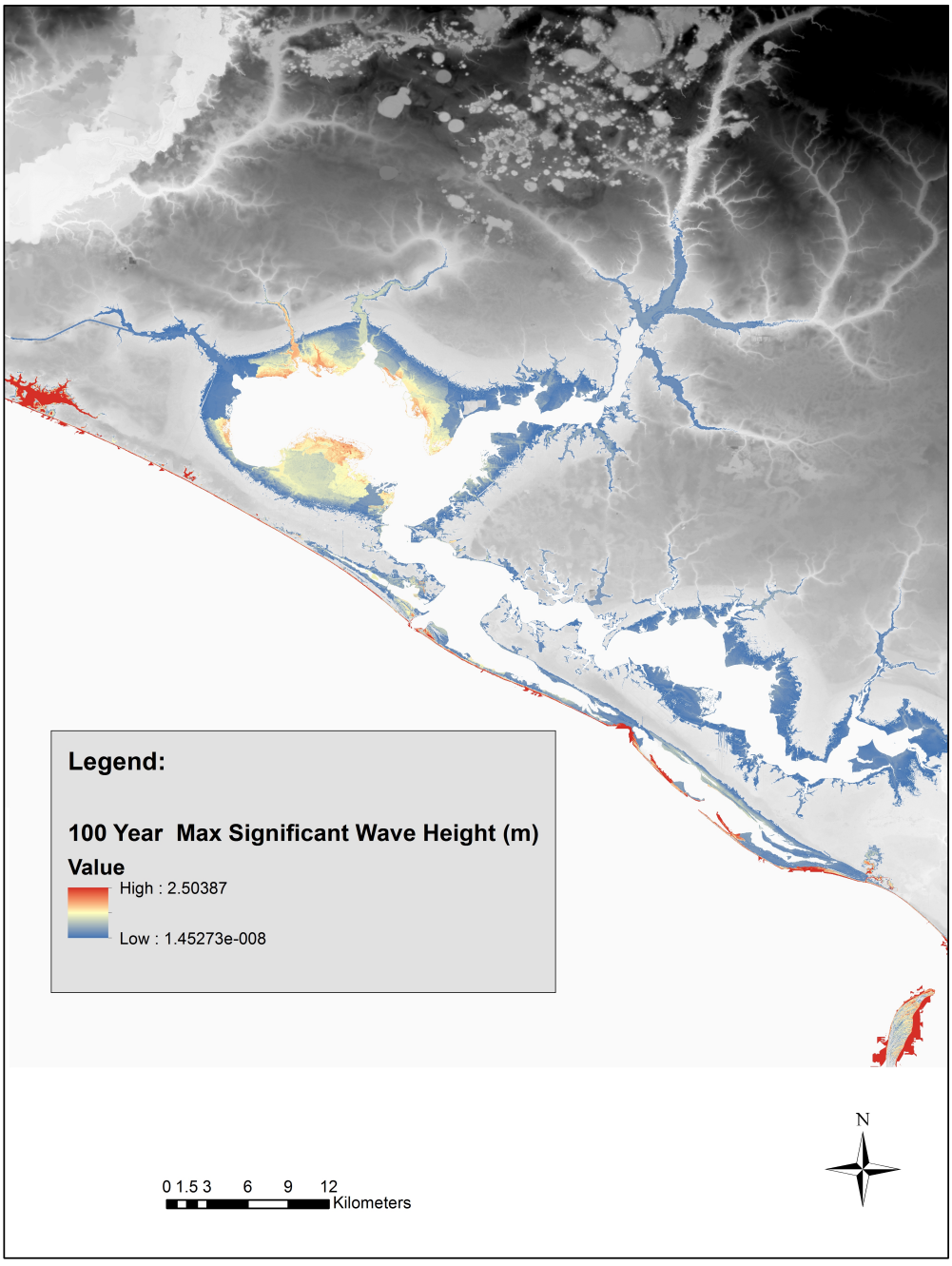

Figure 5.7 Spatial map of 100-year maximum significant wave height over land areas for Panama City, FL.

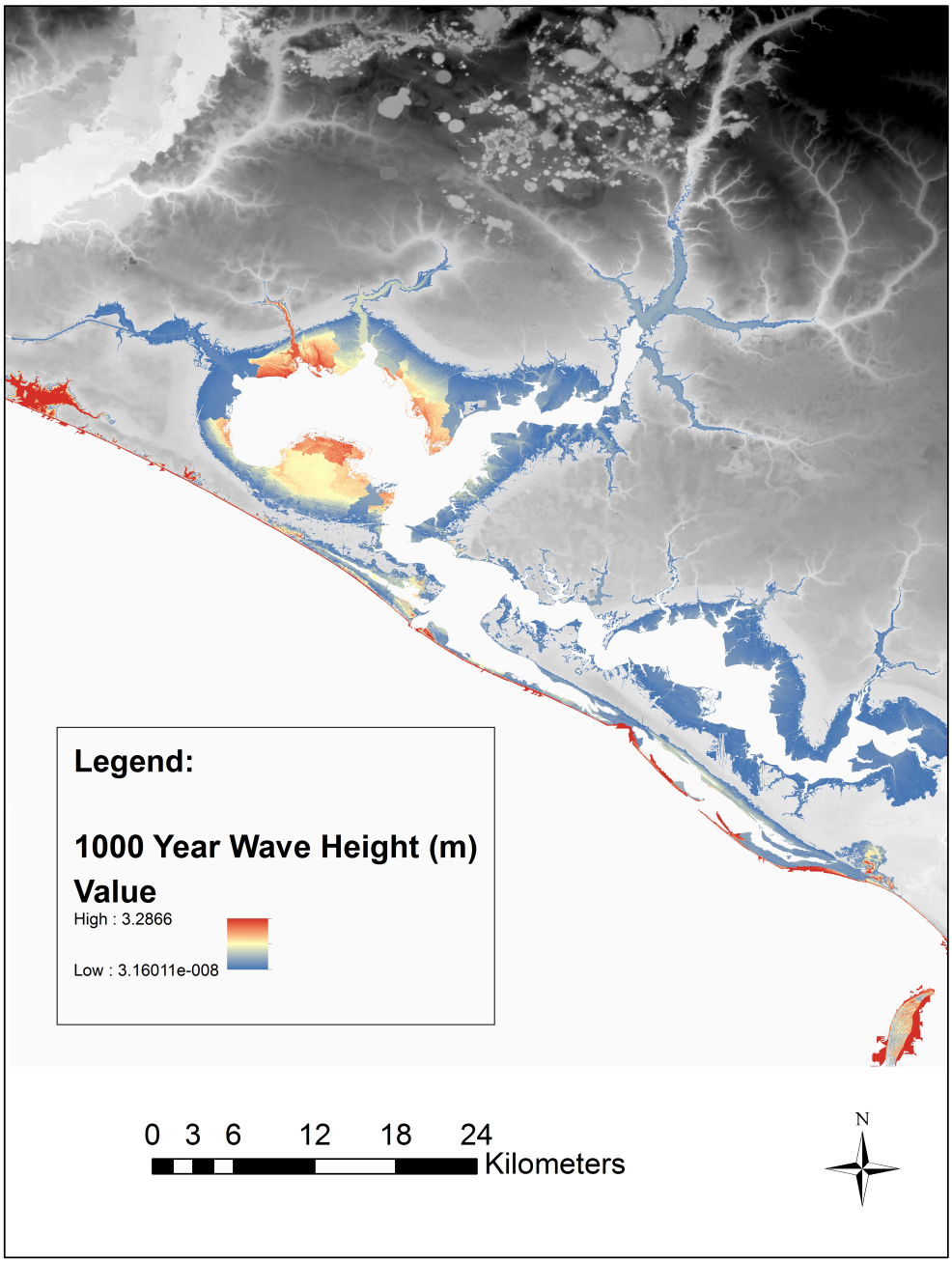

Figure 5.8 Spatial map of 1000-year maximum significant wave height over land areas for Panama City, FL.

6. SUMMARY AND CONCLUSIONS

Simulation of hurricanes via coupled ADCIRC-SWAN and ADCIRC-STWAVE model runs yielded the basis for WRF formulation and JPM-OS application. Non-dimensional equations were developed that parameterized hurricane forced maximum significant wave heights, and curve fitting was done based on landfall position. Over prediction of wave heights via the non-dimensional method illustrated the need for a cap on wave heights. A fully developed sea state cap based on Verhagen and Young (1996) and Breugem and Holthuijsen (2007) was added to the WRF methodology. Bay stations rely on a combination of the non-dimensional equations and fully developed cap, while open coast stations rely solely upon the fully developed cap. When compared to model results, the WRF formulation mostly yielded RMSE errors less than 0.3 m and 20% error. Despite the varying topography, bathymetry, and bottom conditions at the three test sites, the WRF method performed similarly well at all locations. Comparison to Taylor (2012) yielded significant improvements and validation using Kennedy et al. (2011) data yielded good results. A more extensive shallow water hurricane wave data set is needed for further validation, as well as bay data.

Implementation of the WRFs to JPM-OS analysis yielded wave return period curves for Panama City, Florida. The parameters used in the JPM-OS formulation were C_p, R, x_o, and θ. Minimum distance to storm track was approximated using a straight line projection of angle θ. Surge must be calculated using the JPM-OS formulation and SRF equations and used as an input as well in order to calculate wave statistics. Extreme

value analysis of waves at Panama City, FL yielded good results at open coast stations. Bay stations, where wave heights have less correlation with storm parameters, are less accurately predicted by the JPM-OS methodology. Using the JPM-OS results, spatially dense predictions of hurricane wave heights over land were made. These rely upon a constant ratio of wave height to water depth throughout each SRF zone.

Using the methods detailed in this thesis, wave heights are parameterized in a computationally efficient manner for use in extreme value analysis. Once extreme value analysis is conducted, maps of different return period storm on land wave heights can easily be made. Given especially catastrophic hurricanes in recent years, and the potential for increased hurricane frequency, hurricane wave generation and damage needs further research. Recommended topics for further research include:

- Addition of climate change parameters into the WRF methodology
- Changes to the parameterization for areas that experience continually low wave heights despite increasing storm intensity.
- Developing wave specific "WRF" zones that more accurately portray the projection of wave heights on land.
- Apply a more sophisticated mechanism for projecting waves onto land. Use Battjes Jansen distribution to account for probabilities of different significant wave heights making their wave onto land.

REFERENCES

Alves, J.H., Tolman, H.L., Chao, Y.Y. (2004). "Forecasting Hurricane-Generated Wind Waves At NOAA/NCEP." *JCOMM Tech. Rep*., 29(1), 1-13.

Arakawa, H.A., and Suda, K. (1953). "Analysis of Winds, Wind Waves, and Swell over the Sea to the East of Japan During the Typhoon of September 26, 1935." *Mon. Weather Rev.*, 81(1), 31-37.

Blake, E.S., Landsea, C.W., Gibney, E.J. (2011). "The Deadliest, Costliest, and Most Intense United States Tropical Cyclones from 1851 to 2010 (and Other Frequently Requested Hurricane Facts)." *NOAA Technical Memorandum NWS NHC-6.,* Washington, DC.

Booij, N., Ris, R.C., Holthuijsen, L.H. (1999). "A Third-Generation Wave Model for Coastal Regions 1. Model Description and Validation." *J. Geophys. Res*., 104(4), 7649-7666.

Bretschneider, C.L. (1957). "Hurricane Design Wave Practices." *J. Watrwy. and Harb. Div.*, 83(1), 1233-1238.

Breugem, W.A., and Holthuijsen, L.H. (2007). "Generalized Shallow Water Wave Growth from Lake George." *J. Waterw. Port. C-ASCE*., 133(3), 173-182.

Carniello, L., D'Alpaos, A., Defina, A. (2011). "Modeling Wind Waves and Tidal Flows in Shallow Micro-Tidal Basins." *Est. Coast. Shelf Sci.,* 92(2), 263-276.

Dietrich, J.C., Westerink, J.J., Kennedy, A., Smith, J., Jensen, R., Zijlema, M., Holthuijsen, L.H., Dawson, C., Luettich, R., Powell, M., Cardone, V., Cox, A., Stone, G., Pourtaheri, H., Hope, M., Tanaka, S., Westerink, L., Westerink, H.., Cobell, Z. (2011). "Hurricane Gustav (2008) Waves and Storm Surge: Hindcast, Synoptic Analysis, and Validation in Southern Lousiana." *Mon. Weather Rev.,* 139(8), 2488-2522.

Dietrich, J.C., Zijlema, M., Westerink, J.J., Holthuijsen, L.H., Dawson, C., Luettich, R.A., Jensen, R.E., Smith, J.M., Stelling, G.S. (2011). "Modeling Hurricane Waves and Storm Surge Using Integrally-Coupled, Scalable Computations." *Coast. Eng.,* 58(1), 45-65.

Dietrich, J.C., Bunya S., Westerink J.J., Ebersole B.A., Smith, J.M., Atkinson, J.H., Jensen, R., Resio, D.T., Luettich, R.A., Dawson, C., Cardone, V.J., Cox, A.T., Powell, M.D., Westerink, H.J. (2010). "A High-Resolution Coupled Riverine Flow, Tide, Wind, Wind Wave, and Storm Surge Model for Southern Louisiana and Mississippi. Part II: Synoptic Description and Analysis of Hurricanes Katrina and Rita." *Mon. Weather Rev.,* 138(1), 378-404.

Dietrich, J.C., Tanaka S., Joannes J., Westerink, J.J., Dawson, C.N., Luettich, R.A., Zijlema, M., Holthuijsen, L.H., Smith, J.M., Westerink, J.G., Westerink, H.J. (2012). "Performance of the Unstructured-Mesh, SWAN+ ADCIRC Model in Computing Hurricane Waves and Surge." *J. Sci. Comp.,* 52(2), 468-497.

Freeman, J.C., Baer, L., Jung, G. (1957). "The Bathystrophic Storm Tide" *J. Mar. Res.,* 16 (1): 12-22.

Hasselmann, D.E., Dunckel M., Ewing J.A. (1980). “Directional Wave Spectra Observed during JONSWAP 1973.” *J. Phys. Oceanogr.,* 10(1), 1264–1280.

Ho, F.P., and Myers, V.A. (1975) “NOAA Tech. Rep. NWS 38.” *NOAA Technical Memorandum.,* Washington, DC.

Holland, G.J. (1980). “An Analytic Model of the Wind and Pressure Profiles in Hurricanes.” *Mon. Weather Rev.,* 108(8), 1212-1218.

Hope, M.E., Westerink J.J., Kennedy A.B., Kerr P.C., Dietrich J.C, Dawson C., Bender C.J., Smith J.M., Jensen R.E., Zijlema M., Holthuijsen, L.H., Luettich R.A., Powell M.D., Cardone VJ, Cox AT, Pourtaheri H, Roberts HJ, Atkinson JH, Tanaka S, Westerink H.J., Westerink L.G., (2013).” Hindcast and Validation of Hurricane Ike (2008) Waves, Forerunner, and Storm Surge.” *J. Geophys. Res.,* 118(1), 4424-4460.

Holthuijsen, L., (2007). *Waves in Oceanic and Coastal Waters*, Cambridge University Press*,* Oxford, UK.

Ijima, T. and Tang F.W. (1966), "Numerical Calculation of Wind Waves in Shallow Water," *Proceedings of Tenth Conference on Coastal Engineering (Tokyo, Japan, September 1966), American Society of Civil Engineers.*, New York, NY .

Irish, J.L., Resio ,D.T, Cialone, M.C. (2009). “A Surge Response Function Approach to Coastal Hazard Assessment. Part 2: Quantification of Spatial Attributes of Response Functions.” *Nat. Haz.,* 51(1), 183-205.

Irish, J.L., Song, Y.K., Chang, K.A. (2011). “Probabilistic Hurricane Surge Forecasting using Parameterized Surge Response Functions.” *Geophys. Res. Lett.,* 38(1), 1-18.

Jonathan, P.J., and Ewans, K.C. (2007). "Uncertainties in Extreme Wave Height Estimates for Hurricane-Dominated Regions." *J. Offshore Mech. Arct. Eng.,* 129(1), 300-307.

Kahma, K.K. (1981). "A Study of the Growth of the Wave Spectrum with Fetch." *J. Phys. Oceanogr.,* 11(1), 1503-1515.

Kahma, K.K. and Calkoen C.J. (1992). "Reconciling Discrepancies in the Observed Growth of Wind-generated Waves." *J. Phys. Oceanogr.,* 22(1), 1389-1405.

King, D., and Shemdin, O. (1978). "Radar Observations of Hurricane Wave Directions." *Coastal Engineering Proceedings,* 1(16). doi:10.9753/icce.v16.

Knabb, R.D., Rhome, J.R., Brown, D.P. (2005). "Tropical Cyclone Report Hurricane Katrina 23-30 August 2005." *National Hurricane Center,* Miami, FL.

Kennedy, A.B., Gravois, U., Brian, Z. (2011). "Observations of Landfall Wave Spectra During Hurricane Ike." *J. Waterw. Port. C-ASCE.,* 237(3), 142-145.

Lawrence, M.B., and Pelissier, J.M. (1981). "Atlantic Hurricane Season of 1980 (Caribbean, Texas)." *Mon. Weather Rev.,* 109(7), 1567-1582.

Luettich, R.A., and Westerink, J.J. (2004). "Formulation and Numerical Implementation of the 2D/3D ADCIRC Finite Element Model Version 44. XX" *University of North Carolina,* Chapel Hill, NC.

Martyr, R.C., Dietrich J.C., Westerink J.J., Kerr P.C., Dawson C., Smith J.M., Pourtaheri H., Powel, H., Van Ledden M., Tanaka, S., Roberts, H..J., Westerink H.J., Westerink, L.G. (2013). "Simulating Hurricane Storm Surge in the Lower Mississippi River under Varying Flow Conditions." *J. Hydraul. Eng.,* 139(1), 492-501.

National Oceanic and Atmospheric Administration (1975). "Hurricane Eloise: A Report to the Administrator." *U.S. Department of Commerce,* Rockville M.D.

National Oceanic and Atmospheric Administration (2012). "Hurricanes in History." *NOAA Technical Memorandum,* Rockville, MD.

Niedoroda, A.W., Resio D.T., Toro G.R., Divoky D., Das H.S., Reed, C.W., (2010). "Analysis of the coastal Mississippi storm surge hazard." Ocean Eng. 37, 82-90.

Ochi, M (2003). "Hurricane Generated Seas". *Elsevier Ocean Engineering Ltd.,* Oxford, UK.

Panchang, V.G., and Dongcheng L. (2006) "Large Waves In The Gulf Of Mexico Caused By Hurricane Ivan." *Bull. Am. Meteorol. Soc.,* 87(4), 481-489

Panchang, V.G., Jeong C.K., Demirbilek Z. (2013). "Analyses of Extreme Wave Heights in the Gulf of Mexico for Offshore Engineering Applications." *J. Offshore Mech. Arct.,* 135(1), 120-135.

Pierson, W.P., and Moskowitz, L. (1964). "A Proposed Spectral Form for Fully Developed Wind Seas Based on the Similarity Theory of S. A. Kitaigorodskii." *J. Geophys. Res.*, 69(24), 5181-5190.

Ris, R.C., Holthuijsen L.H., Booij, N. (1999). “A Third-Generation Wave Model for Coastal Regions 2. Verification.” *J. Geophys. Res.,* 104(4), 7667-7681.

Resio, D.T., Irish, J.L. Cialone, M.C. (2009). “A Surge Response Function Approach to Coastal Hazard Assessment Part 1: Basic Concepts.” *Nat. Haz.,* 51(1), 163-182.

Resio, D.T., Irish, J.L., Westerink, J.J., Powell N.J. (2013). "The Effect of Uncertainty on Estimates of Hurricane Surge Hazards." *Nat. Haz.,* 66(1), 1443-1459.

Rogers, R., Aberson, S., Black, M., Black, P., Cione, J., Dodge, P., Dunion, J., Gamache, J., Kaplan, J., Powell, M., Shay, N., Surgi, N., Uhlhorn, E. (2006). “The Intensity Forecasting Experiment: A NOAA Multiyear Field Program for Improving Tropical Cyclone Intensity Forecasts.” *Bull. Am. Meteorol. Soc.,* 87(1), 1523-1537.

Song, Y.K., Irish, J.L., Udo, I.E. (2012). “Regional Attributes of Hurricane Surge Response Functions for Hazard Assessment.” *Nat. Haz.,* 64(2), 1475-1490.

Taylor, G., and Hebert, P.J. (1978). “The Deadliest, Costliest, and Most Intense United States Hurricanes of the Century (and other Frequently Requested Hurricane Facts).” *NOAA Technical Memorandum NWS NHC 7,* Washington, DC.

Taylor, S.A. (2012). “Parameterization of Maximum Wave heights Forced by Hurricanes.” *Dissertation, Texas A&M University*., College Station, TX.

Thompson, E.F., and V.J. Cardone (1996) “Practical Modeling of Hurricane Surface Wind Fields.” *J. Waterw. Port. C-ASCE.,* 122(4), 195-205.

Tomzik, T., Kennedy A., Rogers, S. (2014). “Collapse Limit State Fragilities of Wood-Framed Residences from Storm Surge and Waves during Hurricane Ike.” *J. Waterw. Port. C-ASCE.,* 140(1), 43-55.

Toro, G.R., Resio D.T., Divoky D., Niedoroda A.W., Reed, C. (2010). "Efficient Joint-Probability Methods for Hurricane Surge Frequency Analysis." *Ocean Eng.,* 37(1), 125-134.

Udoh, I. (2013). "Robust Hurricane Surge Response Functions." *Dissertation, Texas A&M University*, College Station, TX.

U.S. Army Coastal Engineering Research Center (1984) "Shore Protection Manual, 4th Edition." *U.S. Government Printing Office,* Washington, DC.

U.S. Army Coastal Engineering Research Center (2001). "STWAVE: Steady-State Spectral Wave Model User's Manual for STWAVE, Version 3.0." *U.S. Government Printing Office,* Washington, DC.

U.S. Census Bureau. (2010). " Summary Population and Housing Characteristics Report." *U.S. Government Printing Office,* Washington, DC.

U.S. Department of Commerce (2006). "Hurricane Katrina Service Assessment Report". *U.S. Government Printing Office,* Washington, DC.

Van Dorn, W.C. (1953). "Wind Stresses on an Artificial Pond." *J. Mar Res.,* 12(1), 249-276.

Walsh, E.J., Hancock, D.W., Hines D.E., Swift R.N., Scott J.F. (1989). "An Observation of the Directional Wave Spectrum Evolution from Shoreline to Fully Developed." *J. Phys. Oceanogr.,* 19(1), 670–690.

Wright, R., 2001. "Wind Energy Development in the Caribbean." *Renew. Energ.,* 24(1), 439-444.

Young, I.R. (1988). "Parametric Hurricane Wave Prediction Model." *J. Waterw. Port. C-ASCE.,* 114(1), 637–652.

Young, I.R., and Verhagen, LA (1996 a). "The Growth of Fetch Limited Waves in Water of Finite Depth 1. Total Energy and Peak Frequency." *Coast. Eng.,* 29(1-2), 47-78.

Young, I.R., and Verhagen, L.A. (1996 b). "The Growth of Fetch Limited Waves in Water of Finite Depth 2. Spectral Evolution." *Coast. Eng.,* 29(1-2), 79-99.

Young, I.R., and Verhagen, L.A. (1996 c). "The Growth of Fetch Limited Waves in Water of Finite Depth 3. Directional Spectra." *Coast. Eng.,* 29(1-2), 101-121.

Young, I.R. (1998). "Observations of the Spectra of Hurricane Generated Waves." *Ocean Eng.,* 25(4–5), 261-276

Young, I.R., (1999). *Wind Generated Ocean Waves*, Elsevier Sciences Ltd*.,* Oxford, UK.

Young, I.R. (2003). "A Review of the Sea State Generated by Hurricanes." *Mar. Struct.,* 16(1), 201-218.

Zijlema, M., (2010). "Computation of Wind-Wave Spectra in Coastal Waters with SWAN on Unstructured Grids." *Coast. Eng.,* 57(1), 267-277.

Zundel, A.K., Cialone, M.A., and Moreland, T.J. (2002). "SMS steering module for coupling waves and currents, 1. ADCIRC and STWAVE," *Coastal and Hydraulics Engineering Technical Note ERDC/CHL CHETN-IV-41, U.S. Army Engineer Research and Development Center,* Vicksburg, MS.